The Role of Quantum Geometry In Some Interacting Systems

Rahul Roy, UCLA

T. S. Jackson, G. Möller and R. Roy, "Geometric stability of topological lattice phases," arXiv:1408.0843 (2014).

R. Roy, "Band geometry of fractional topological insulators," *Phys. Rev. B* **90**, 075104 (2014).

S. A. Parameswaran, R. Roy and S. L. Sondhi, "Fractional Chern insulators and the W_∞ algebra," *Phys. Rev. B* **85**, 241308 (2012).

The Hall effect

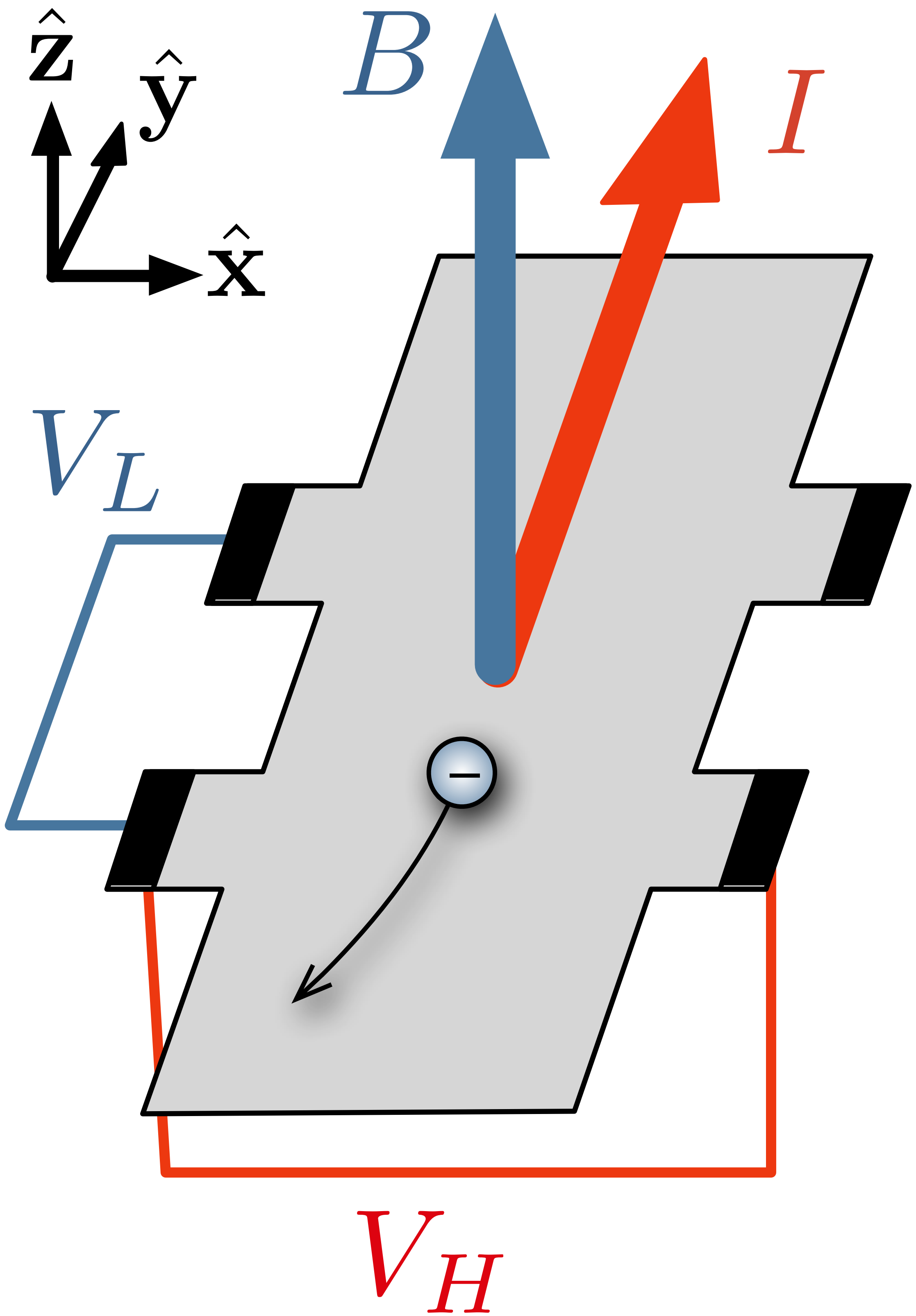

Hall 1879: Charge transport in metals due to *negatively* charged particles.

The Hall effect

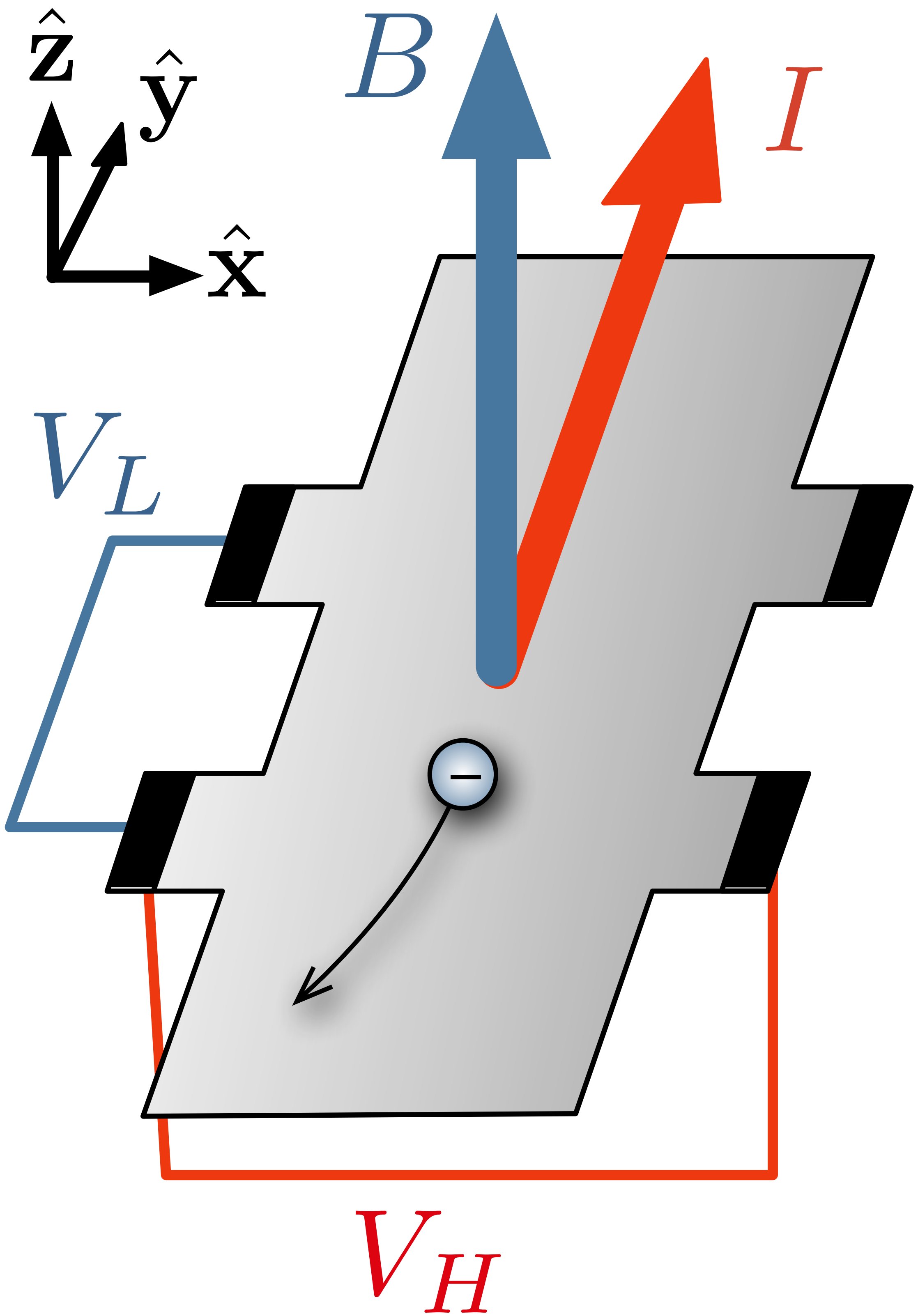

Franklin c. 1780s: Single-fluid theory of electricity; positive and negative charge.

Hall 1879: Charge transport in metals due to *negatively* charged particles.

Thompson 1897: Identification of electron as a fundamental particle from measurement of *e/m*.

The *integer quantum* Hall effect

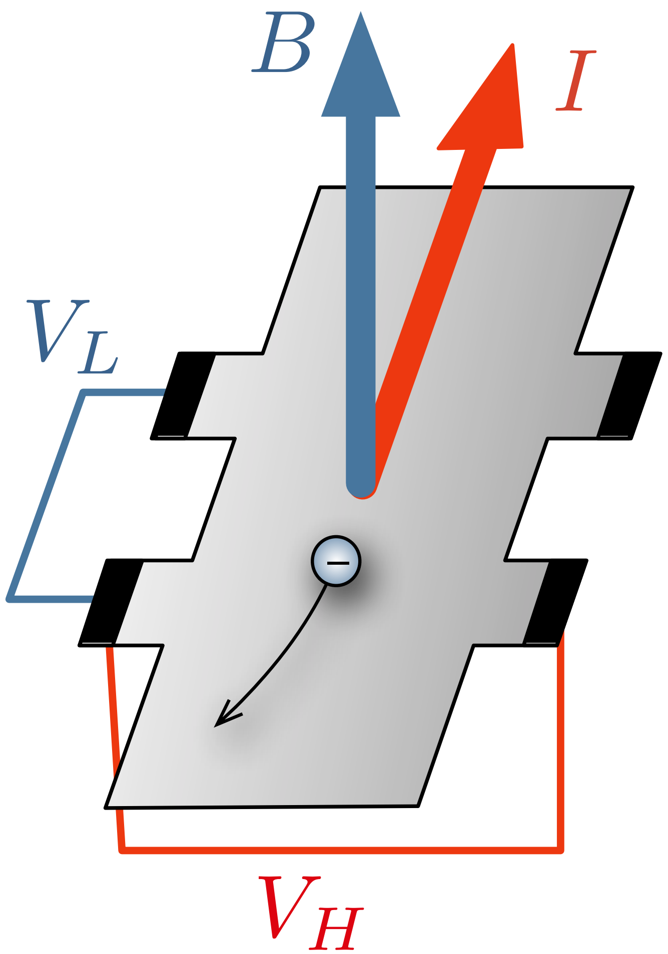

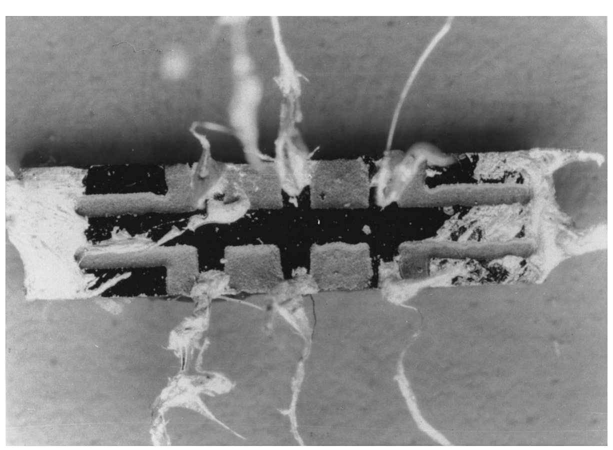

From Stormer, RMP ***71****, 875*

Landau level filling fraction $\nu = n_e \frac{\Phi_0}{B}$

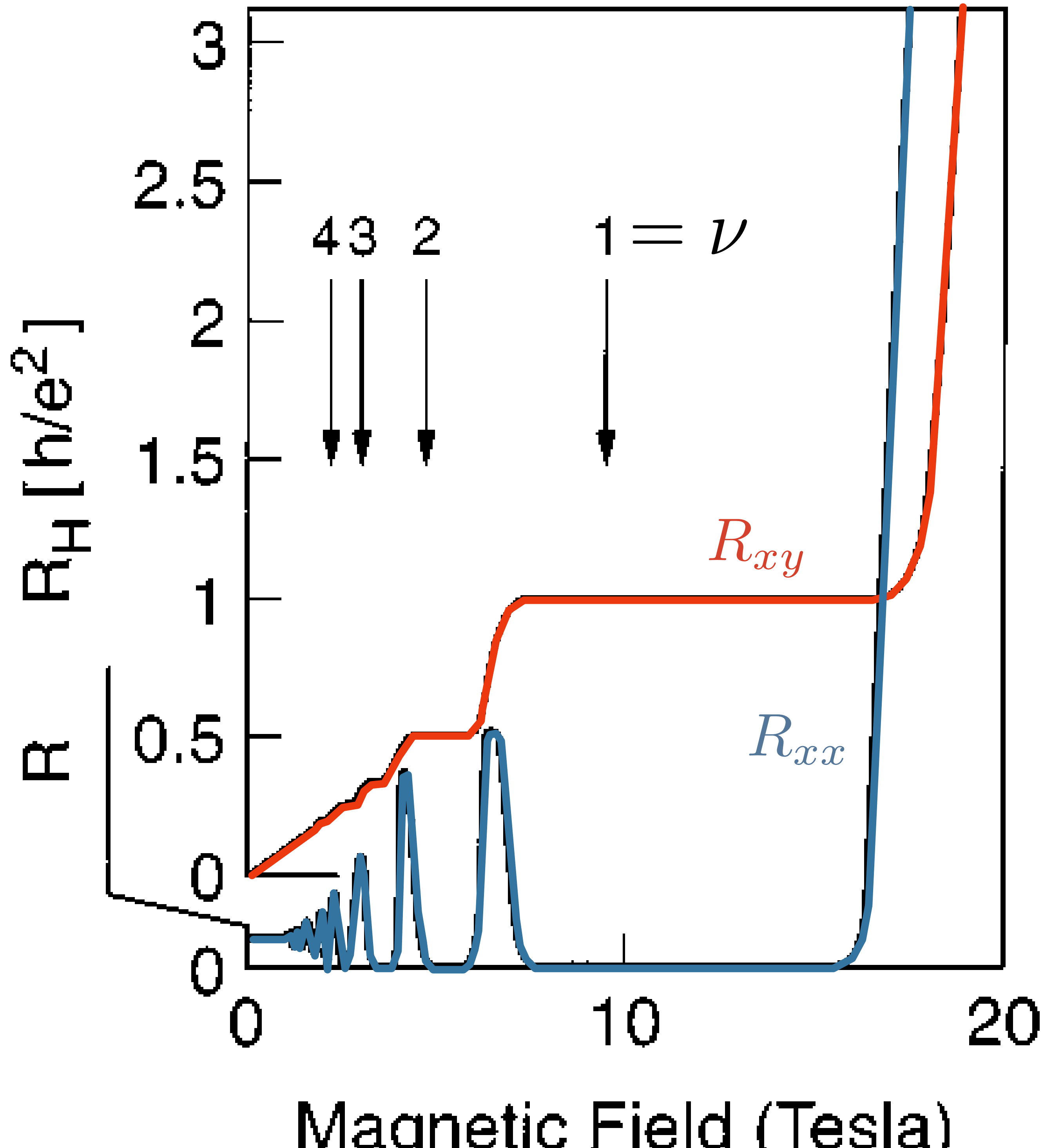

From Stormer, RMP ***71****, 875*

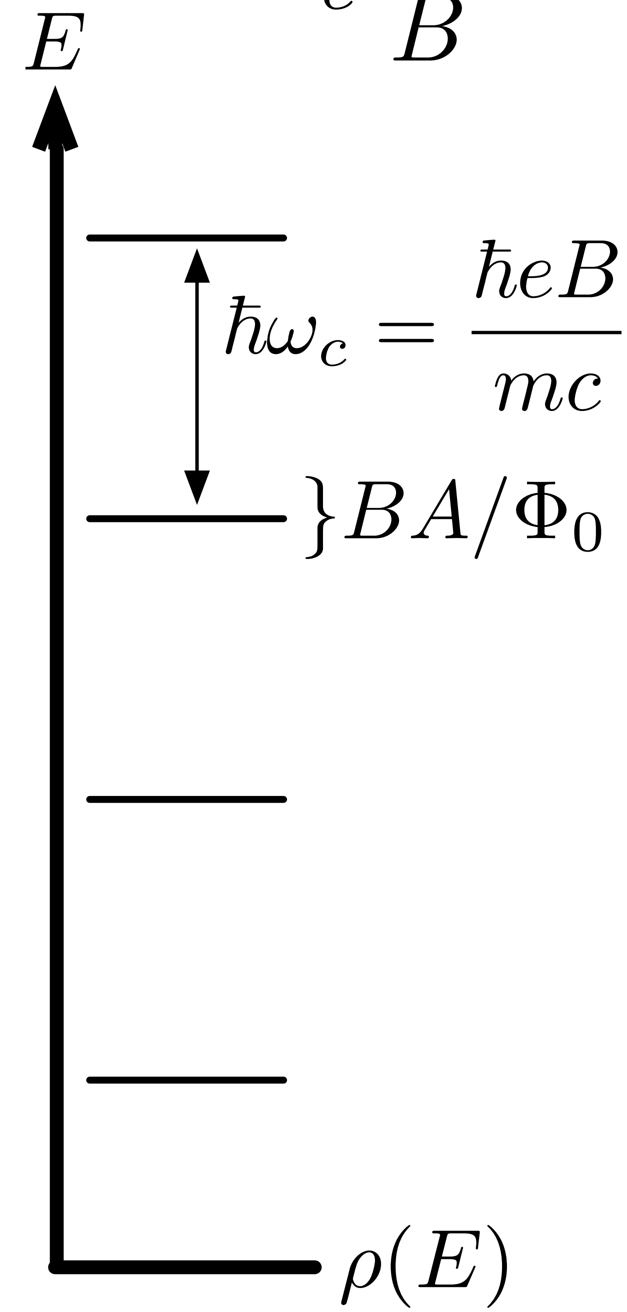

The *integer quantum* Hall effect

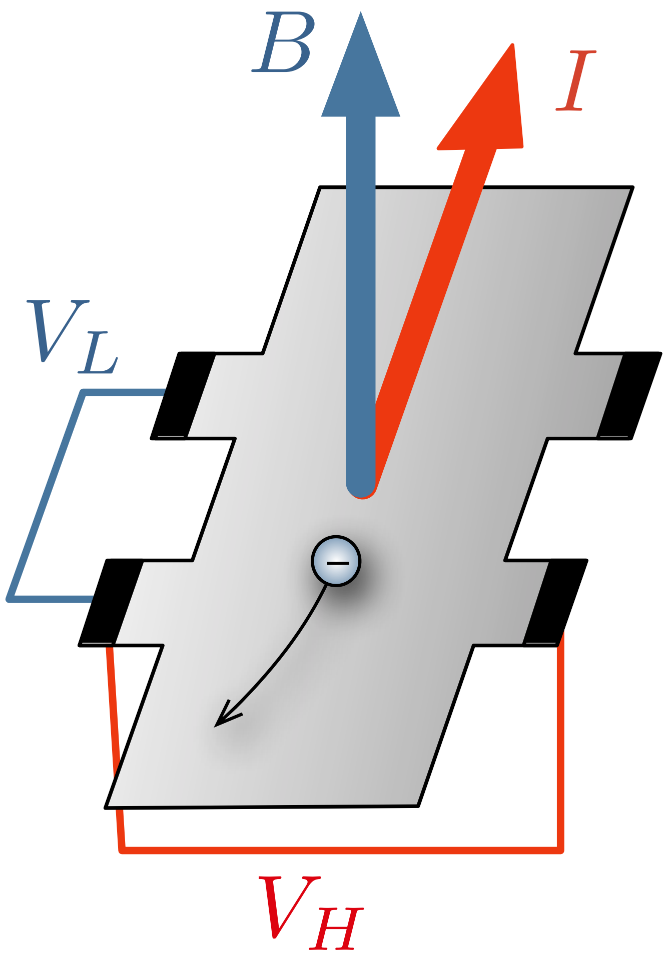

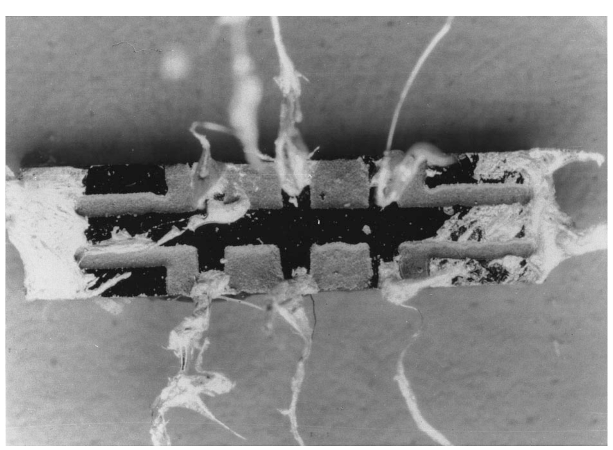

From Stormer, RMP **71**, 875

Landau level filling fraction $\nu = n_e \frac{\Phi_0}{B}$

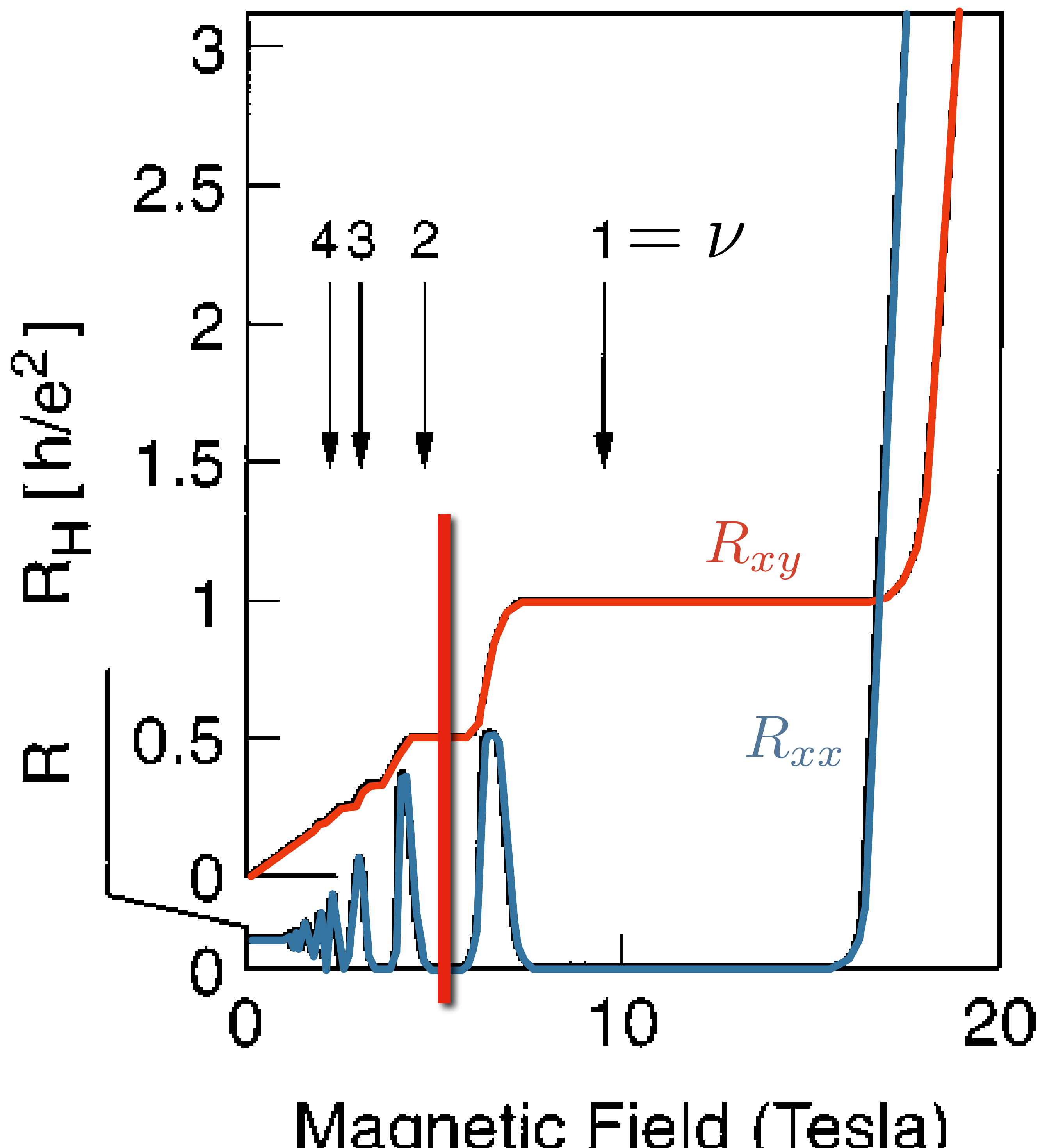

From Stormer, RMP **71**, 875

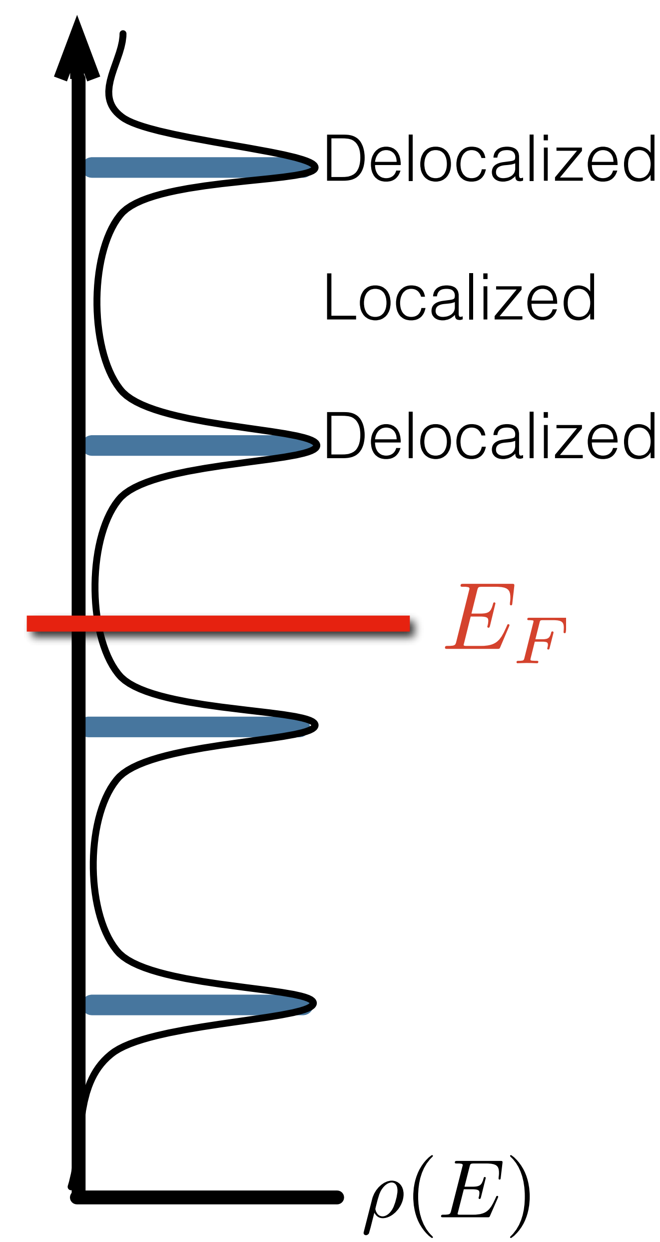

The *integer quantum* Hall effect

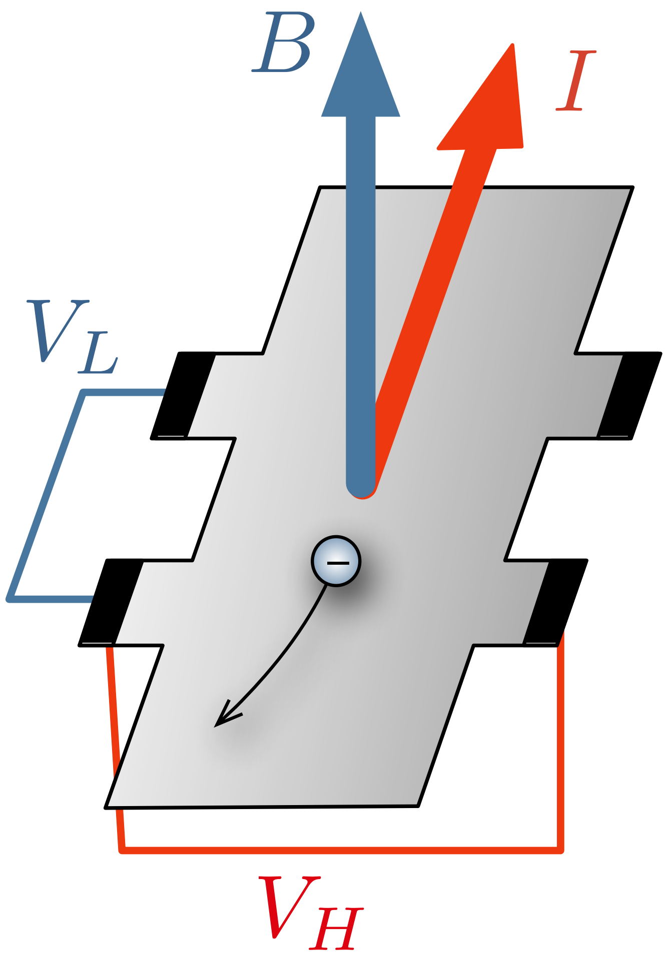

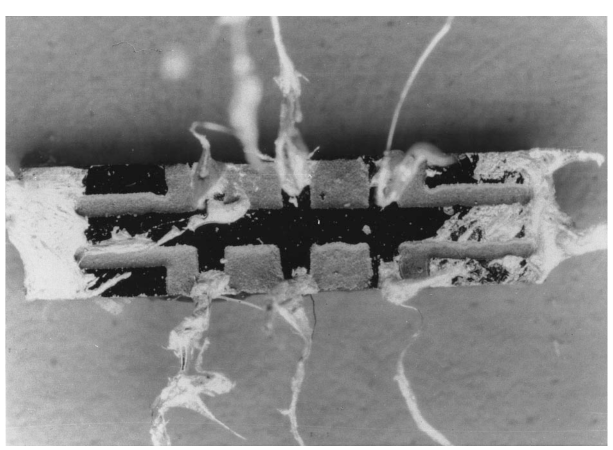

*From Stormer, RMP **71**, 875*

Landau level filling fraction $\nu = n_e \frac{\Phi_0}{B}$

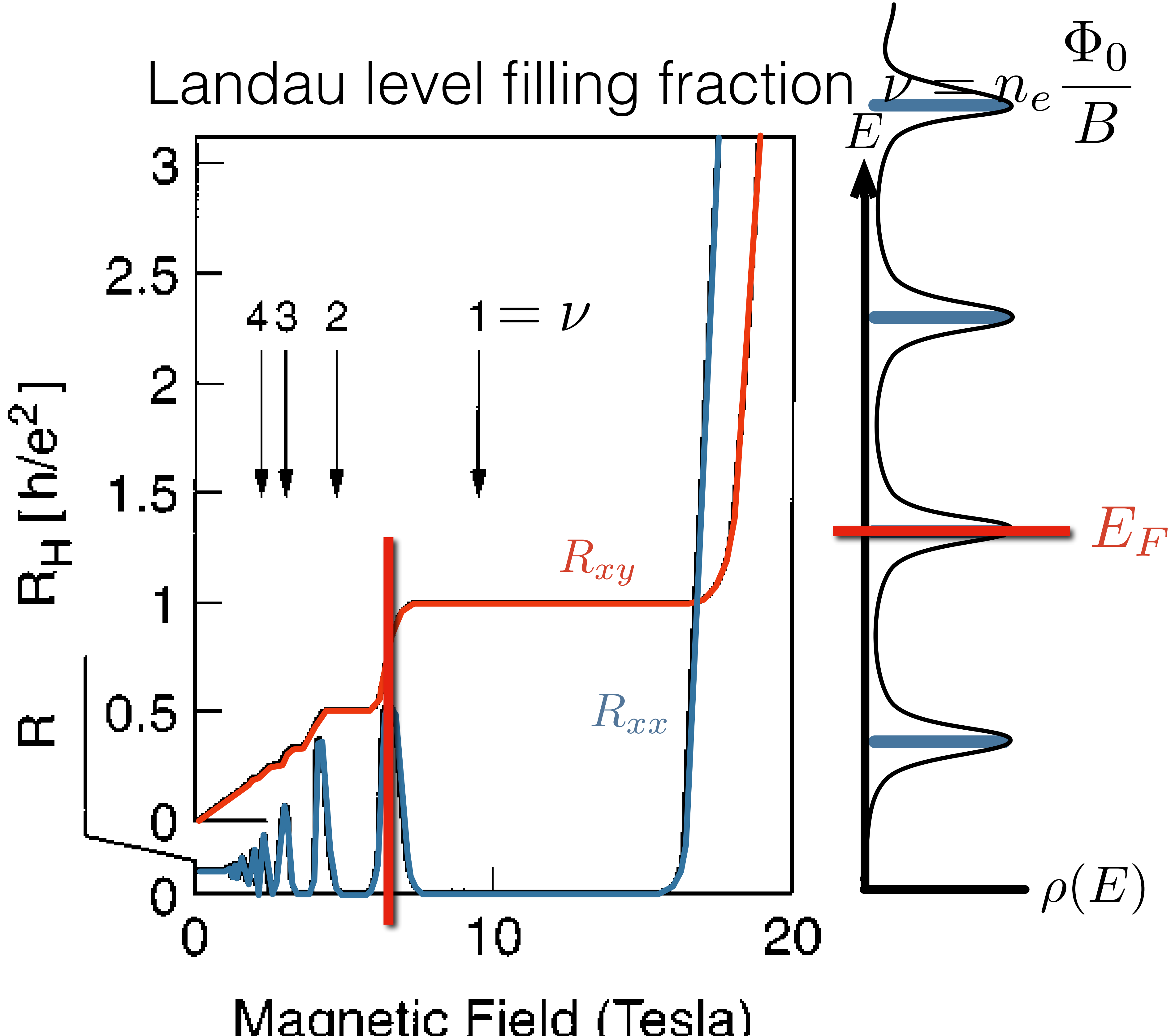

*From Stormer, RMP **71**, 875*

The *integer quantum* Hall effect

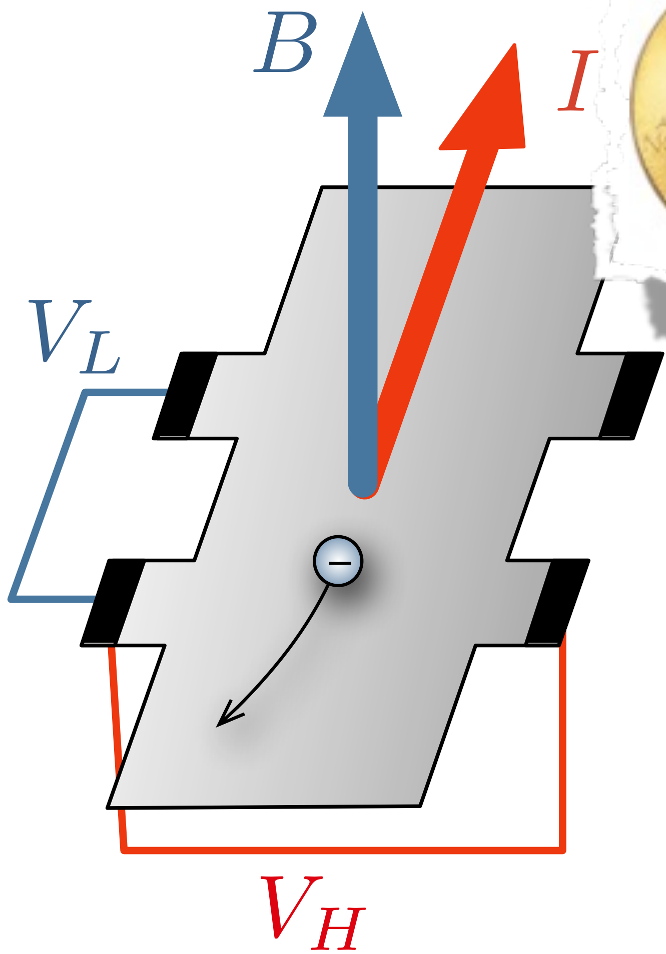

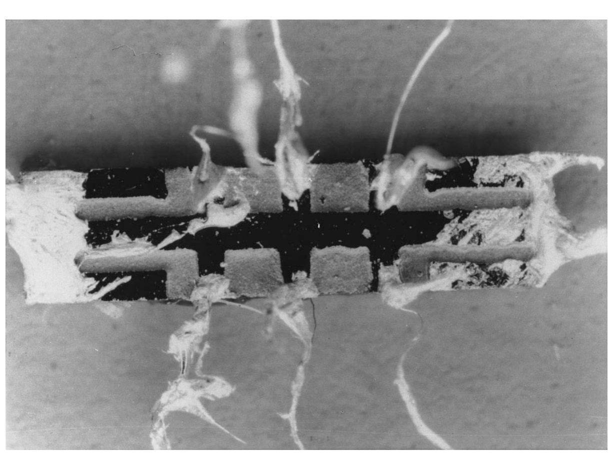

From Stormer, RMP **71**, 875

First QHE Nobel:
v. Klitzing '85

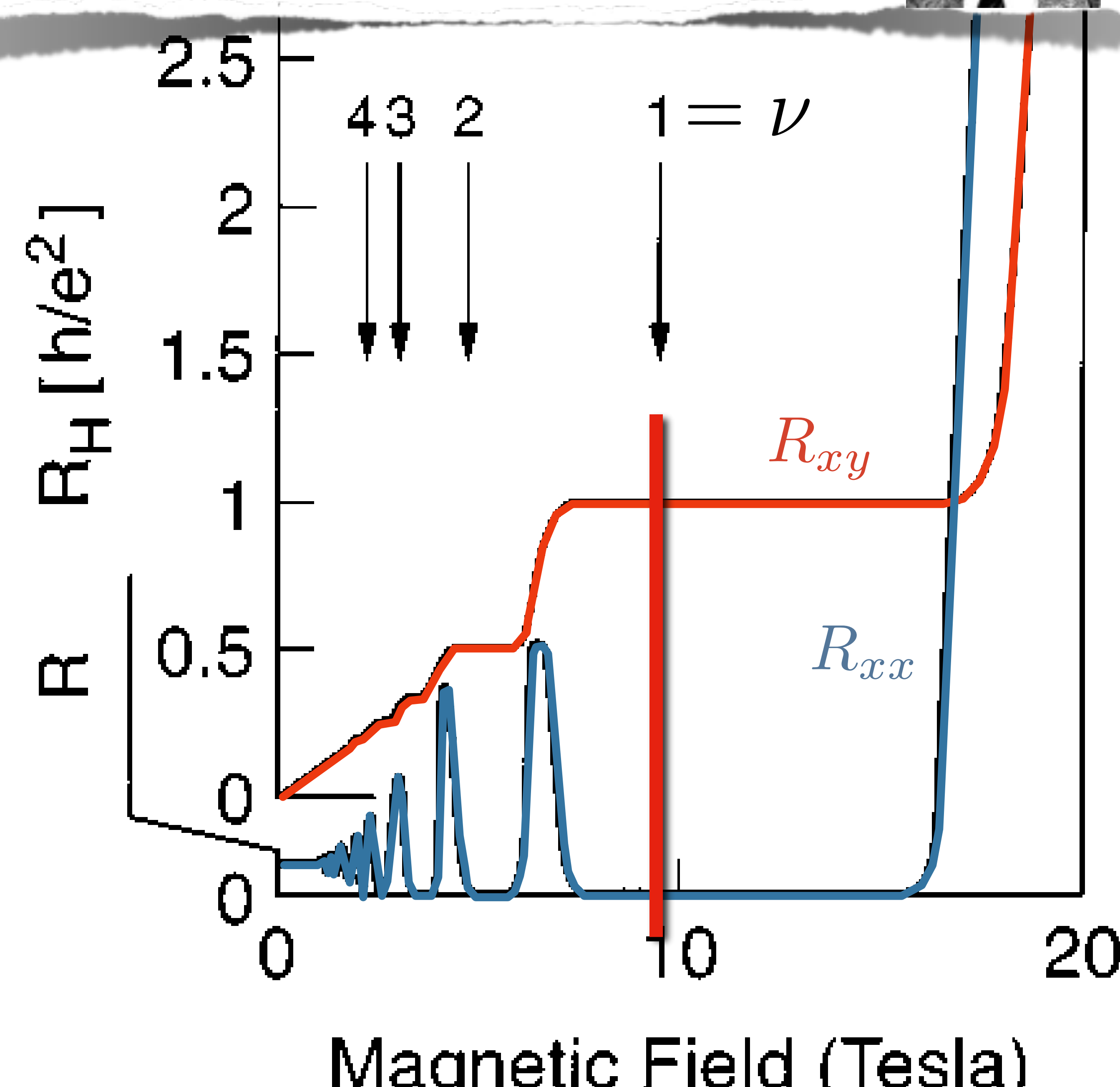

From Stormer, RMP **71**, 875

$$\nu = n_e \frac{\Phi_0}{B}$$

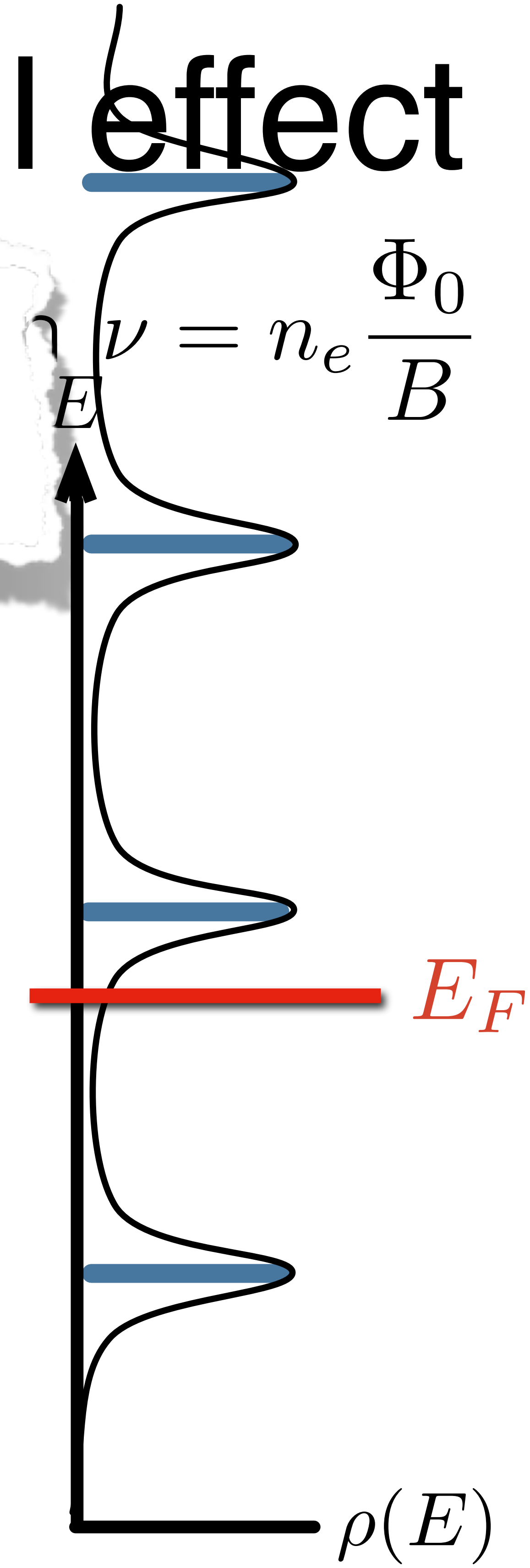

The *fractional* quantum Hall effect*s*

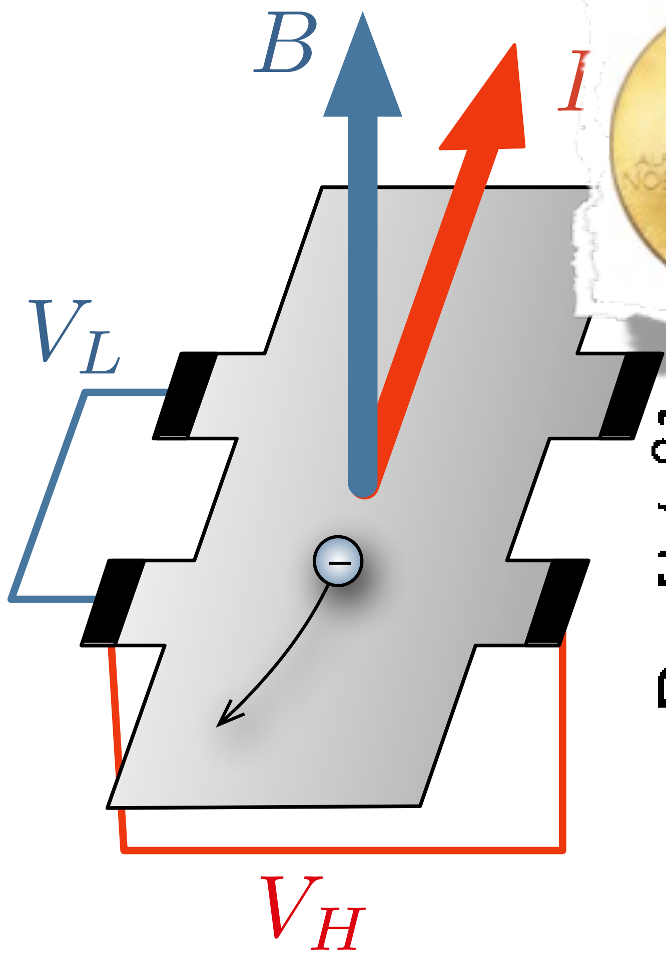

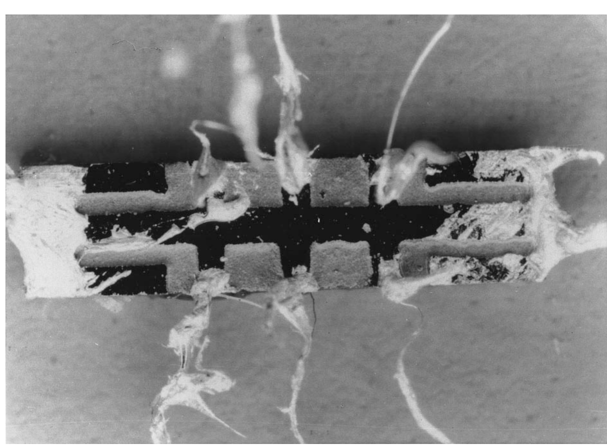

From Stormer, RMP **71**, 875

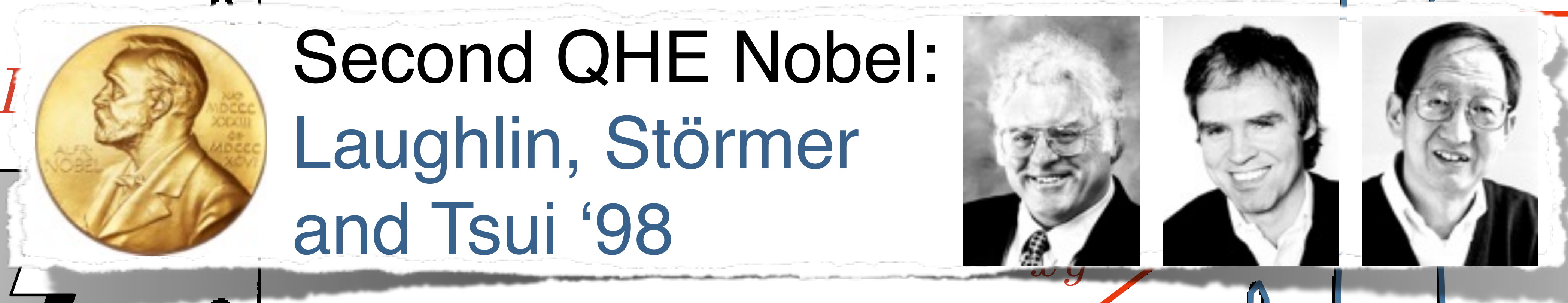

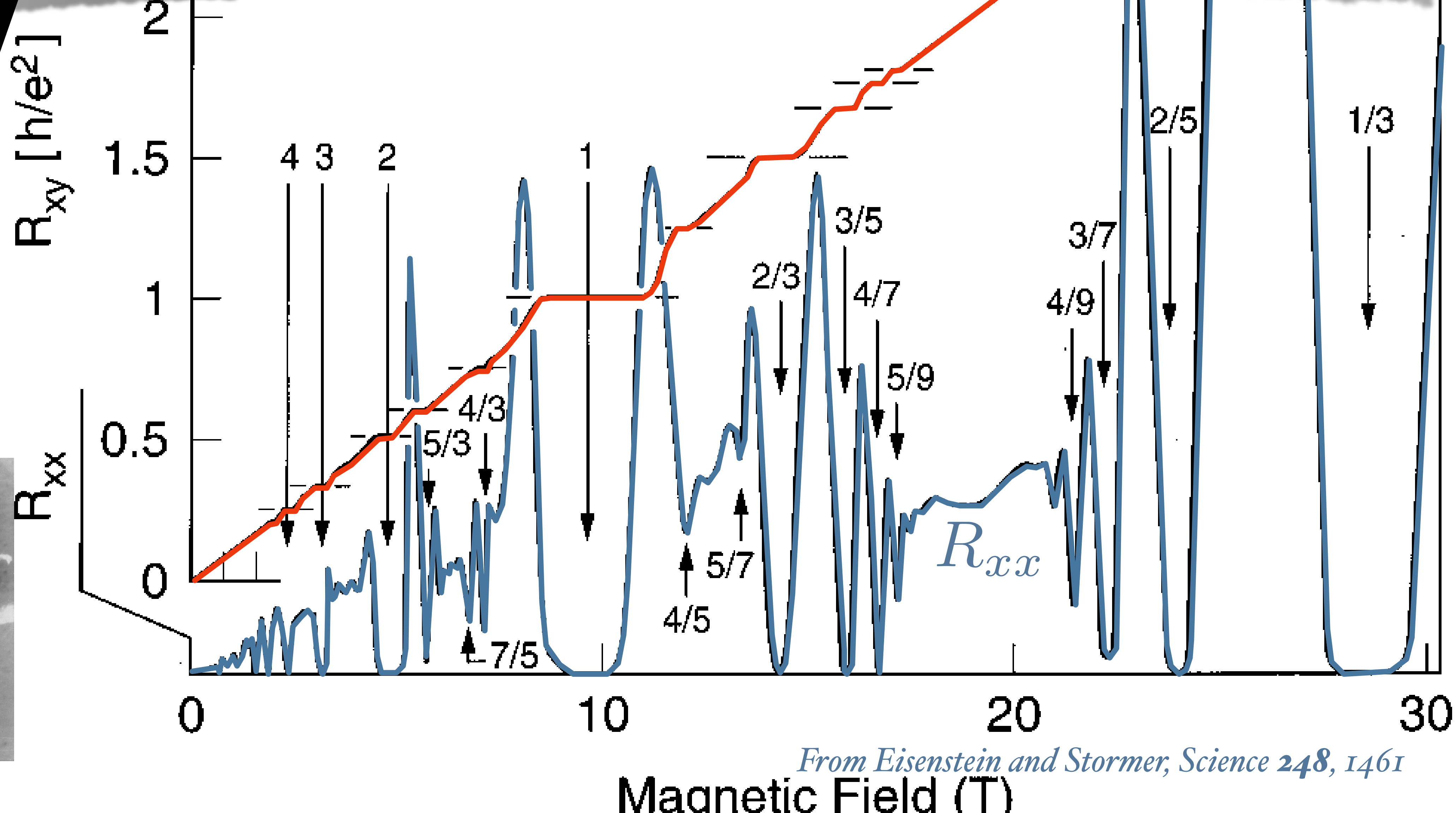

From Eisenstein and Stormer, Science **248**, 1461

Low-energy effective theory is a Chern-Simons TQFT

$$\mathcal{L} = \frac{1}{4\pi}\alpha_I K_{IJ}\varepsilon\partial\alpha_J + \frac{1}{2\pi}At_I\varepsilon\partial\alpha_I + \alpha_I j_I$$ (Abelian case)

- Zhang, Hansson and Kivelson '89; López and Fradkin '91; others: Chern-Simons as effective hydrodynamics of FQHE. Here following Wen and Zee '92.

Chern-Simons TQFT describes ground state, charge and braiding statistics of low-lying excitations.

Hall conductance: $\sigma = \nu = \sum_{I,J} t_I (K^{-1})_{IJ} t_J$

A conglomerate of l_J particles of type J has charge

$$q = \sum_{IJ} t_I (K^{-1})_{IJ} l_J$$

and statistics $\frac{\theta}{\pi} = \sum_{I,J} l_I (K^{-1})_{IJ} l_J$

$$\Psi_{w_1,w_2} = e^{i\theta}\Psi_{w_2,w_1}$$

$$\vec{\Psi}_{w_1,w_2} = U\vec{\Psi}_{w_2,w_1}$$

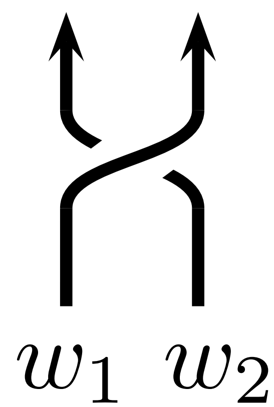

Nonabelian anyonic statistics: braiding matrices can't be simultaneously diagonalized! ex: Majorana modes.

Potential application: topologically protected quantum computing

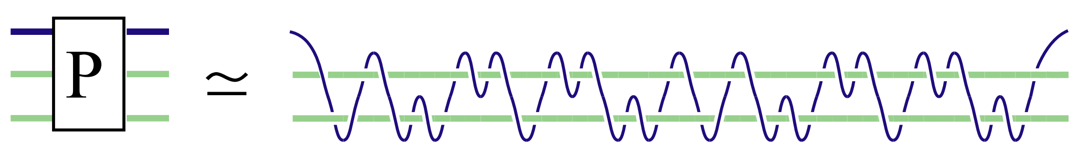

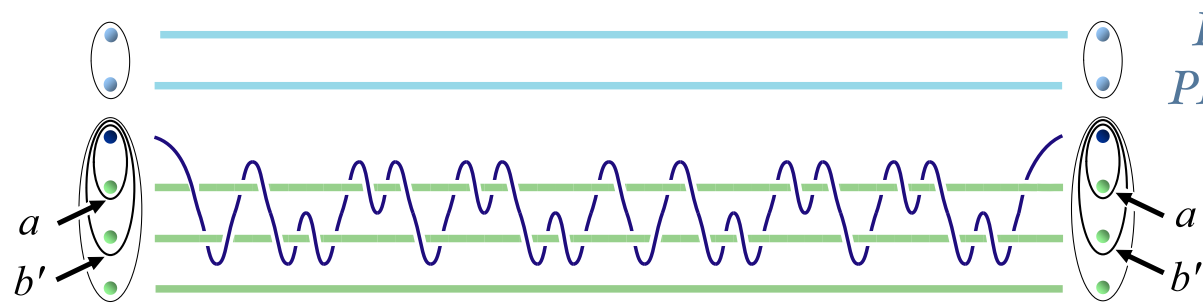

*From Hormozi et al, PRB **75**, 165310 (2007)*

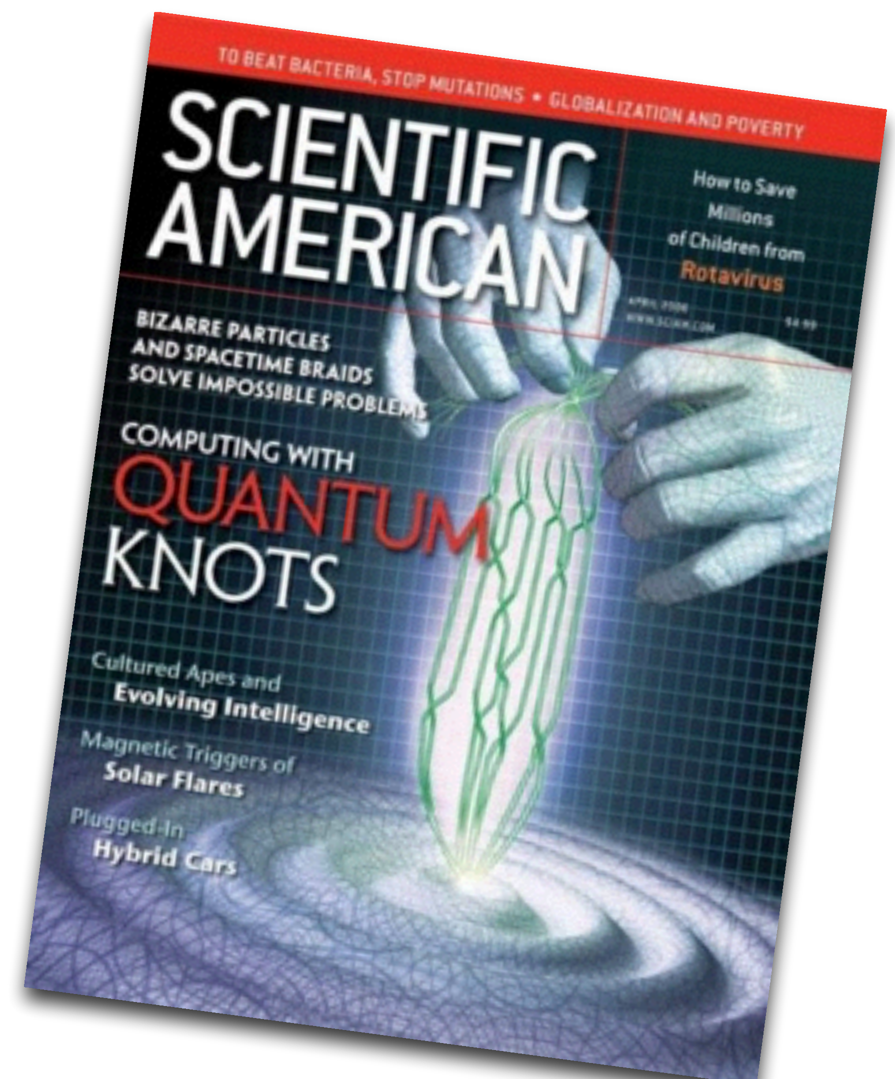

Fractional Topological Insulators: What are they and why do we care?

- Numerical evidence for existence of topologically ordered states in fractionally filled Chern bands.

- One might think that they are a simple extension of the FQHE states. However, Chern bands look very different from Landau levels.

- Several approaches suggested to resolve this problem:
    - Wavefunctions : Qi; Wu, Bernevig and Regnault;Liu & Bergholtz; Scaffidi & Moller, Lee, Thomale & Qi
    - Partons : McGreevy et al; Lu & Ran
    - Density algebras : Parameswaran, Roy & Sondhi; Roy; Murthy Shankar

Fractional Topological Insulators: What are they and why do we care?

- *Many* proposals for tight-binding models with topologically nontrivial bands.

Tang, Mei and Wen, PRL **106**, 236802 (2011)
Sun et. al., PRL **106**, 236803 (2011)
Neupert et. al., PRL **106**, 236804 (2011)
Hu, Kargarian and Fiete, PRB **84**, 155116 (2011)
Sheng et. al., Nat. Comm. **2**, 389 (2011)

Regnault and Bernevig, PRX **1**, 021014 (2011)
Wang et. al. PRL **107** 146803 (2011)
Wu, Bernevig and Regnault, PRB **85**, 075116 (2012)
Bernevig and Regnault, PRB **85** 075128 (2012)
Wang et. al. PRL **108**, 126805 (2012)
Venderbos et. al. PRL **108** 126405 (2012)

Basic notation:

$$H_0 = \sum_{i,j,a,b} t_{ij}^{ab} c_{i,a}^{\dagger} c_{j,b}$$

$$H_0 = \sum_{\mathbf{k},a,b} c_{\mathbf{k},a}^{\dagger} h_{ab}(\mathbf{k}) c_{\mathbf{k},b}$$

The corresponding eigenstates are given by

$$|\mathbf{k}, \alpha\rangle = \gamma^{\dagger}_{\mathbf{k},\alpha}|0\rangle \equiv \sum_{a} u^{\alpha}_{a}(\mathbf{k}) c^{\dagger}_{\mathbf{k},a}|0\rangle$$

and in terms of these band operators, the Hamiltonian is

$$H_0 = \sum_{\alpha=1}^{\mathcal{N}} \epsilon_{\alpha}(\mathbf{k}) \gamma^{\dagger}_{\mathbf{k},\alpha} \gamma_{\mathbf{k},\alpha}$$

Flatten bands:

$$h_{ab}(\mathbf{k}) \to \tilde{h}_{ab}(\mathbf{k}) = h_{ab}(\mathbf{k})/\epsilon_1(\mathbf{k})$$

Full Hamiltonian:

$$H = H_0 + V$$

H_0 is the flat topological band Hamiltonian.

Interactions of the generalized Hubbard form:

$$V = \frac{1}{2}\sum_{i,j} U_{ij}\hat{n}_i\hat{n}_j$$

Berry curvature and connection:

$$\vec{\mathcal{A}}_\alpha(\mathbf{k}) = i \sum_{b=1}^{\mathcal{N}} u_b^{\alpha *}(\mathbf{k}) \vec{\nabla}_{\mathbf{k}} u_b^\alpha(\mathbf{k}).$$

$$\mathcal{B}_\alpha(\mathbf{k}) = \vec{\nabla}_{\mathbf{k}} \times \vec{\mathcal{A}}_\alpha(\mathbf{k})$$

$$C_\alpha = \frac{1}{2\pi} \int_{\mathrm{BZ}} d^2k \, \mathcal{B}_\alpha(\mathbf{k})$$

Flattened Hamiltonians

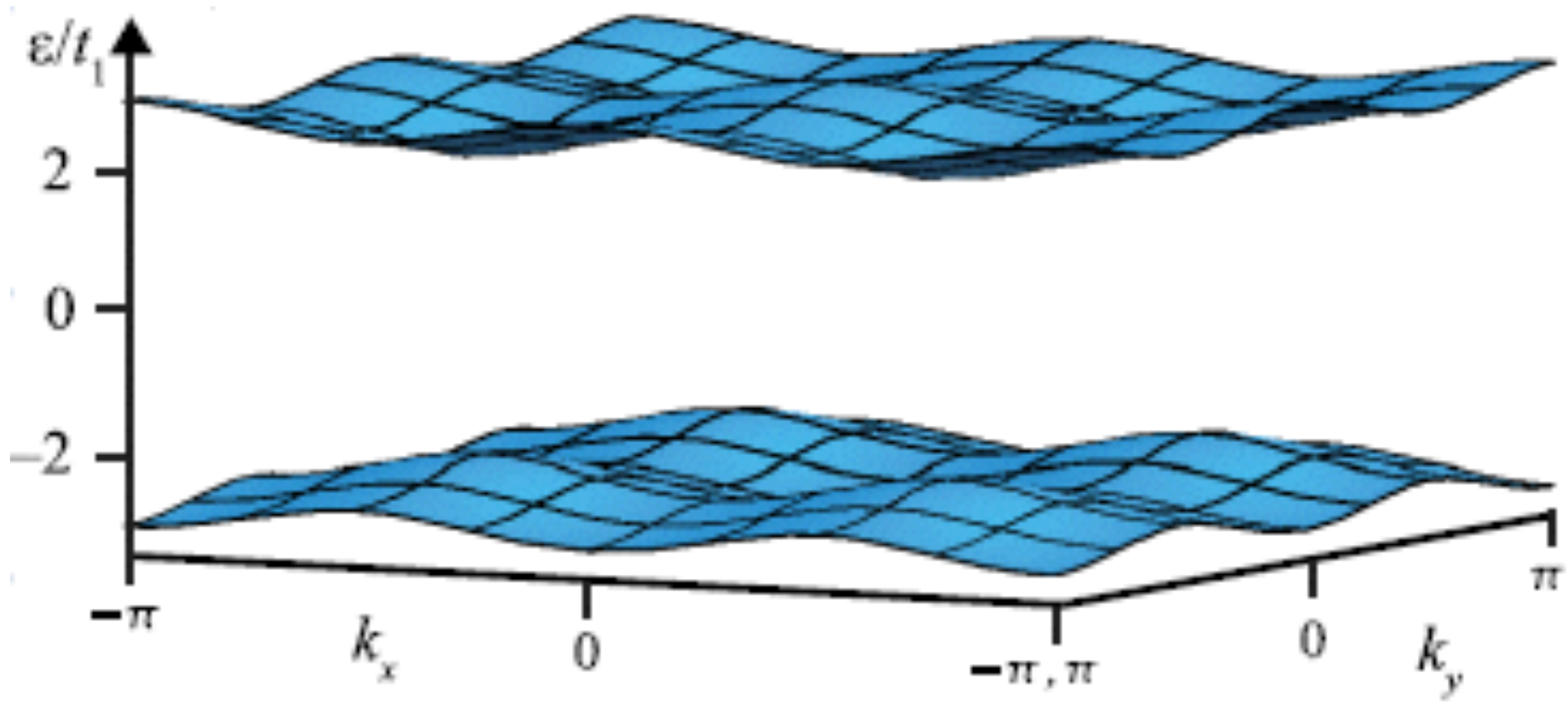

$$H_0 = \sum_{\mathbf{k},a,b} c^\dagger_{\mathbf{k},a} h_{ab}(\mathbf{k}) c_{\mathbf{k},b} \qquad h(\mathbf{k}) = d_0(\mathbf{k})\sigma_0 + \mathbf{d}(\mathbf{k}).\sigma$$

$$h^{\mathrm{flat}}(\mathbf{k}) := \frac{h(\mathbf{k})}{\epsilon_-(\mathbf{k})}$$

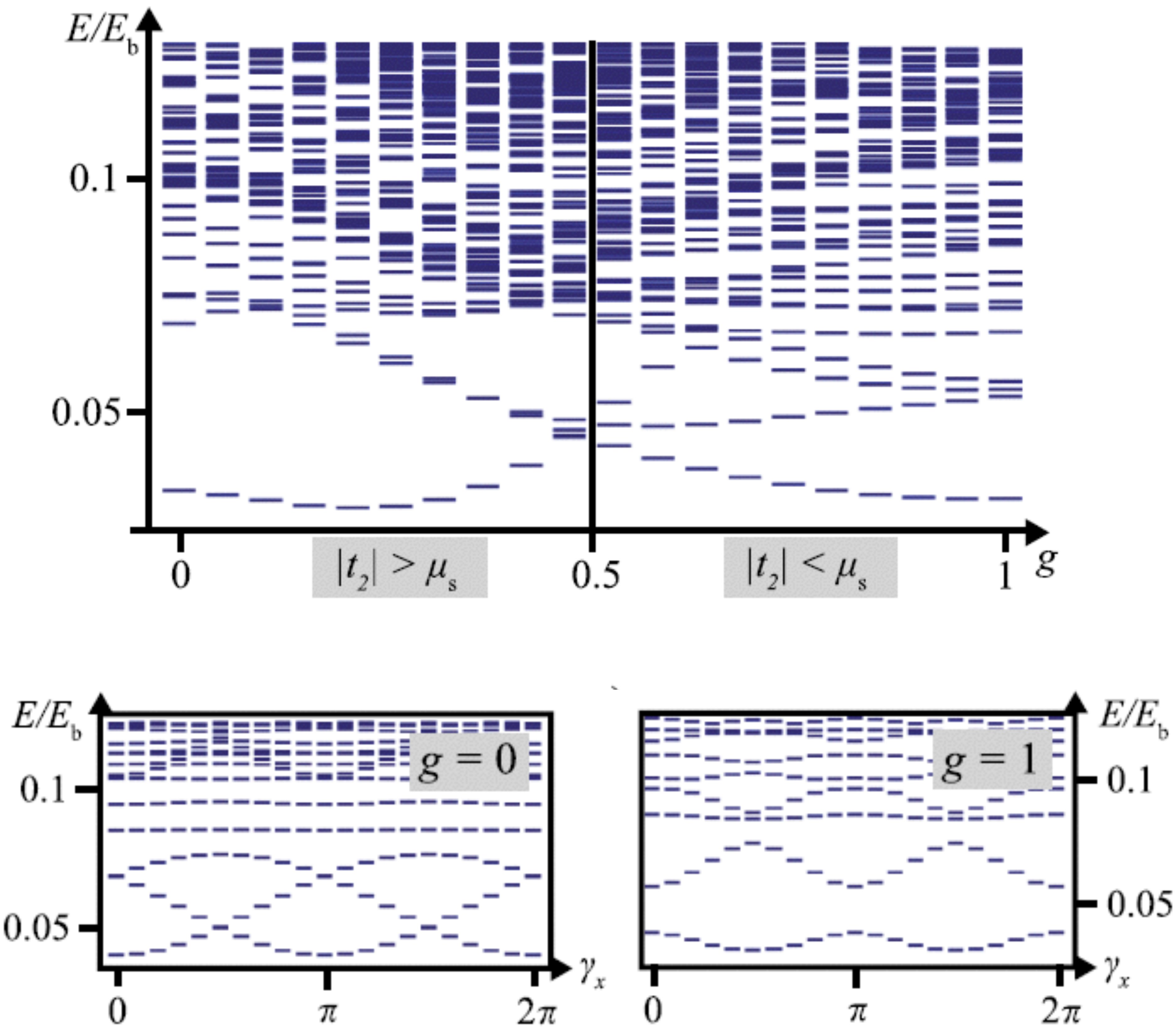

E/E_b
0.1
0.05
0
0.5
1
g
|t_2| > μ_s
|t_2| < μ_s
E/E_b
0.1
0.05
g = 0
0
π
2π
γ_x
E/E_b
0.1
0.05
g = 1
0
π
2π
γ_x

Sheng et al (Nature Comm. 2,389 (2011))

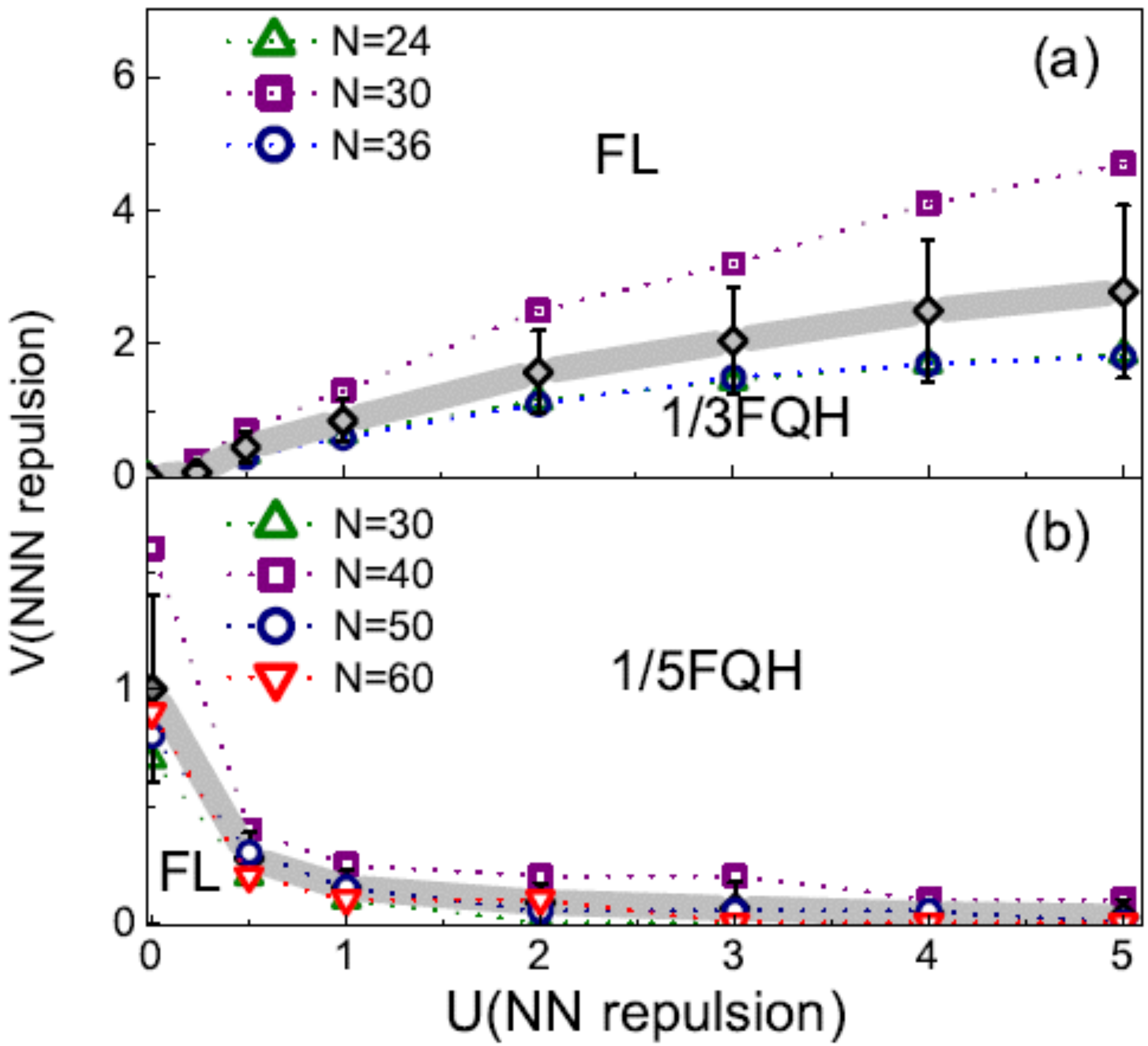

Evidence of ground-state degeneracy

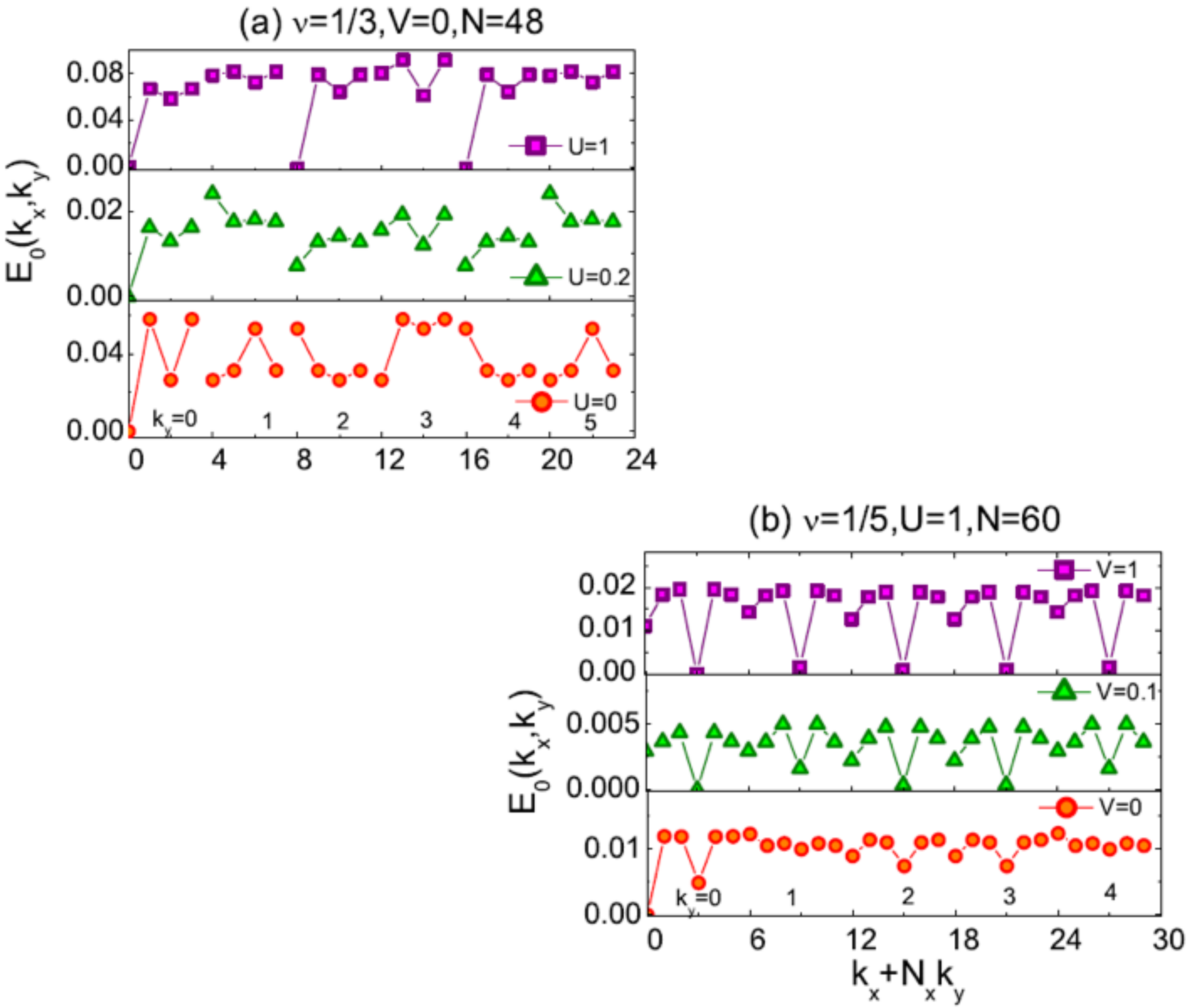

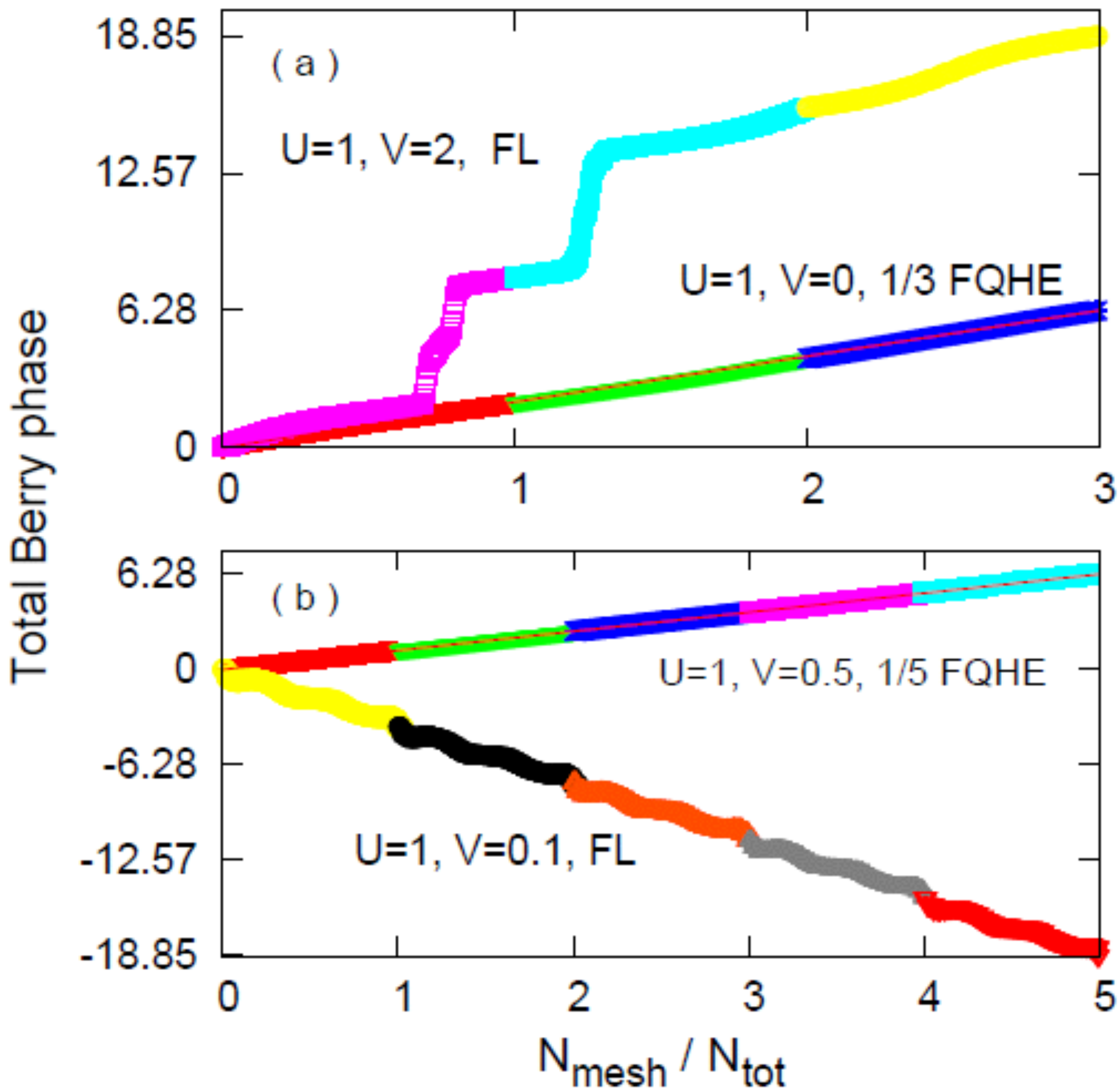

Total Berry phase
18.85
12.57
6.28
0
(a)
U=1, V=2, FL
U=1, V=0, 1/3 FQHE
0
1
2
3
6.28
0
-6.28
-12.57
-18.85
(b)
U=1, V=0.5, 1/5 FQHE
U=1, V=0.1, FL
0
1
2
3
4
5
N_mesh / N_tot

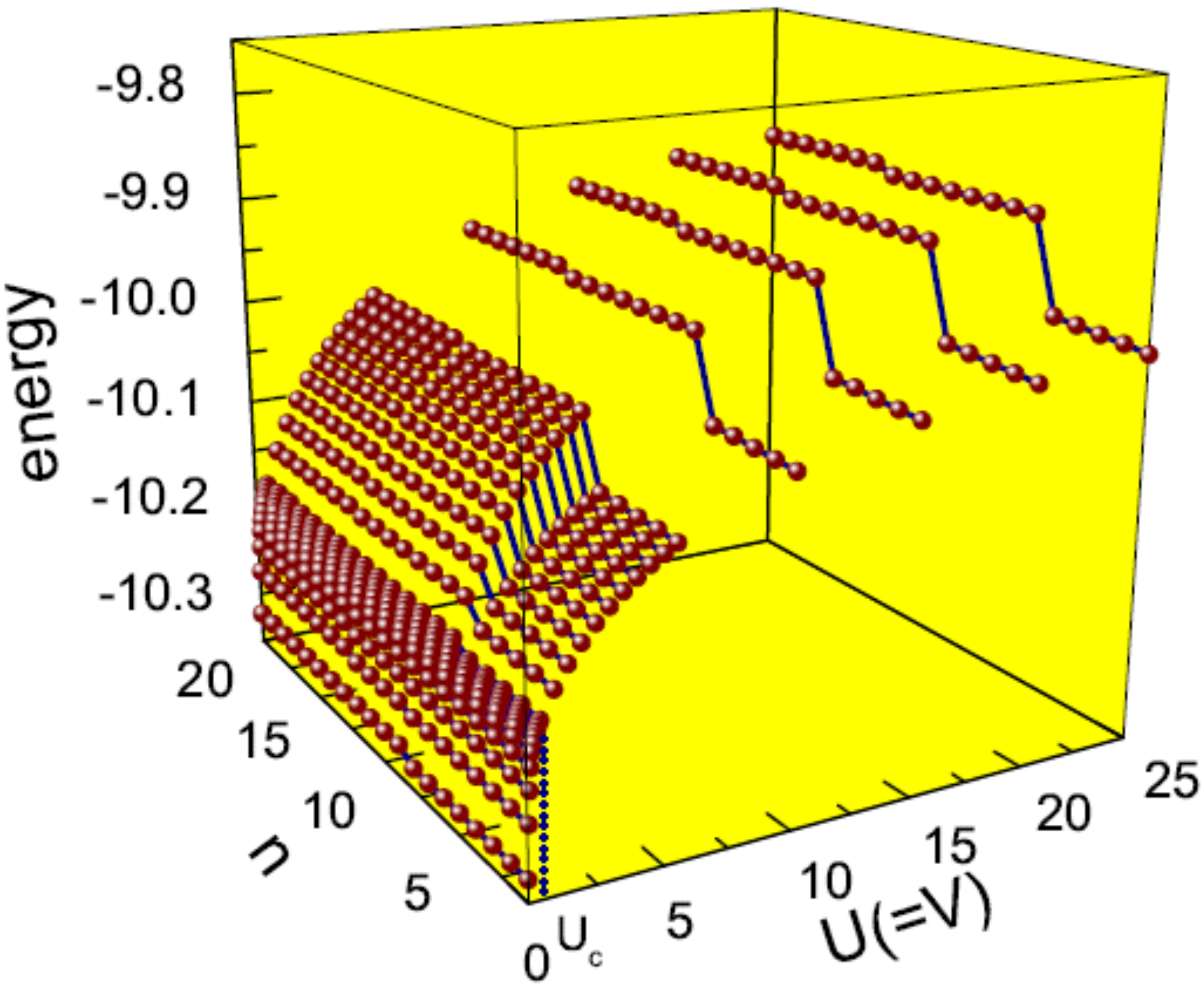

energy
-9.8
-9.9
-10.0
-10.1
-10.2
-10.3
n
20
15
10
5
0
U_c
5
10
15
20
25
U(=V)

Short-distance physics in FQHE

from Wen and Zee,
PRB **46**, 2290 (1992)

this subject. The long-distance physics of the quantum topological fluids is described in general by the Lagrangian in (2+1)-dimensional space time[7]

$$\mathcal{L} = \frac{1}{4\pi} \sum_{I,J} \alpha_I K_{IJ} \varepsilon \partial \alpha_J + \cdots \, . \tag{1.1}$$

We use the compact notation $\alpha \varepsilon \partial \beta \equiv \varepsilon^{\mu\nu\lambda} \partial_\nu \beta_\lambda$ for two gauge potentials α_μ and β_μ. The ellipses in (1.1) represent short-distance physics about which this formalism has nothing to say. If the matrix K does not have any zero ei-

- Short-distance physics — details of band structure, interactions, etc.— is vital to the stability of an FCI.

Short-distance physics in FQHE

- Short-distance physics — details of band structure, interactions, etc.— is vital to the stability of an FCI.

Haldane model,
Fermionic Laughlin state

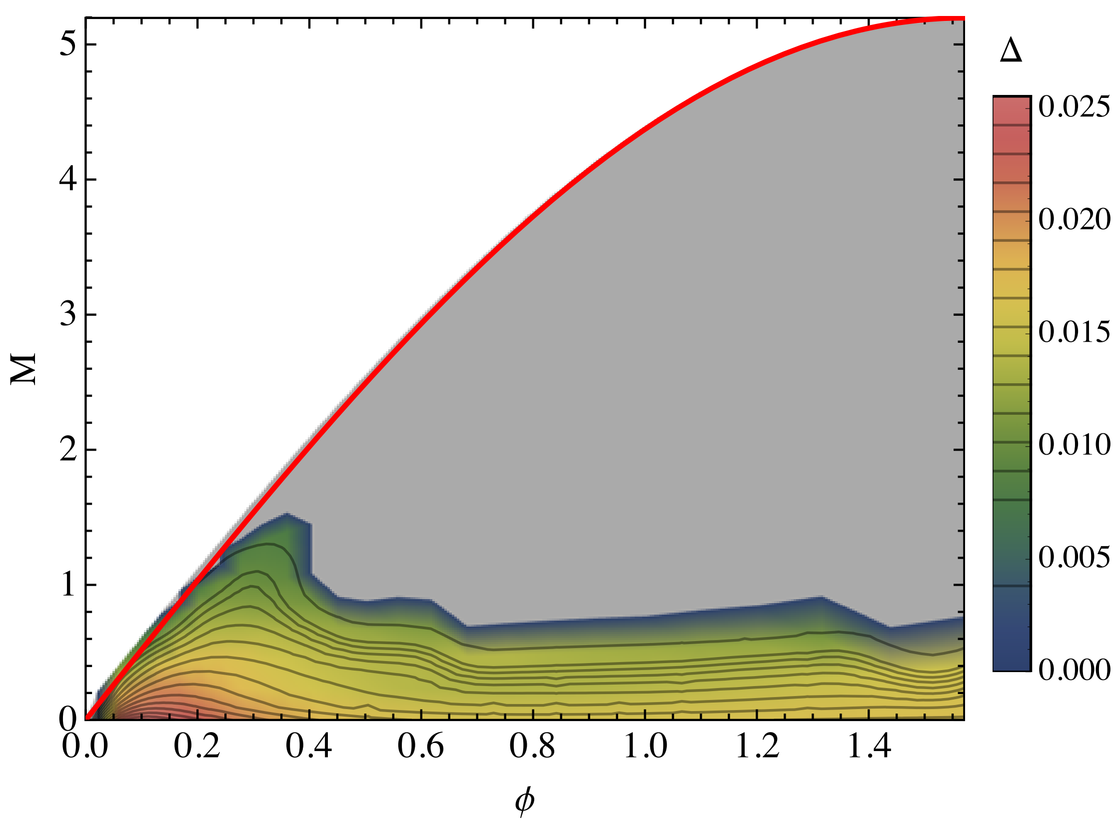

Haldane model w/ extra hopping,
bosonic Moore-Read state

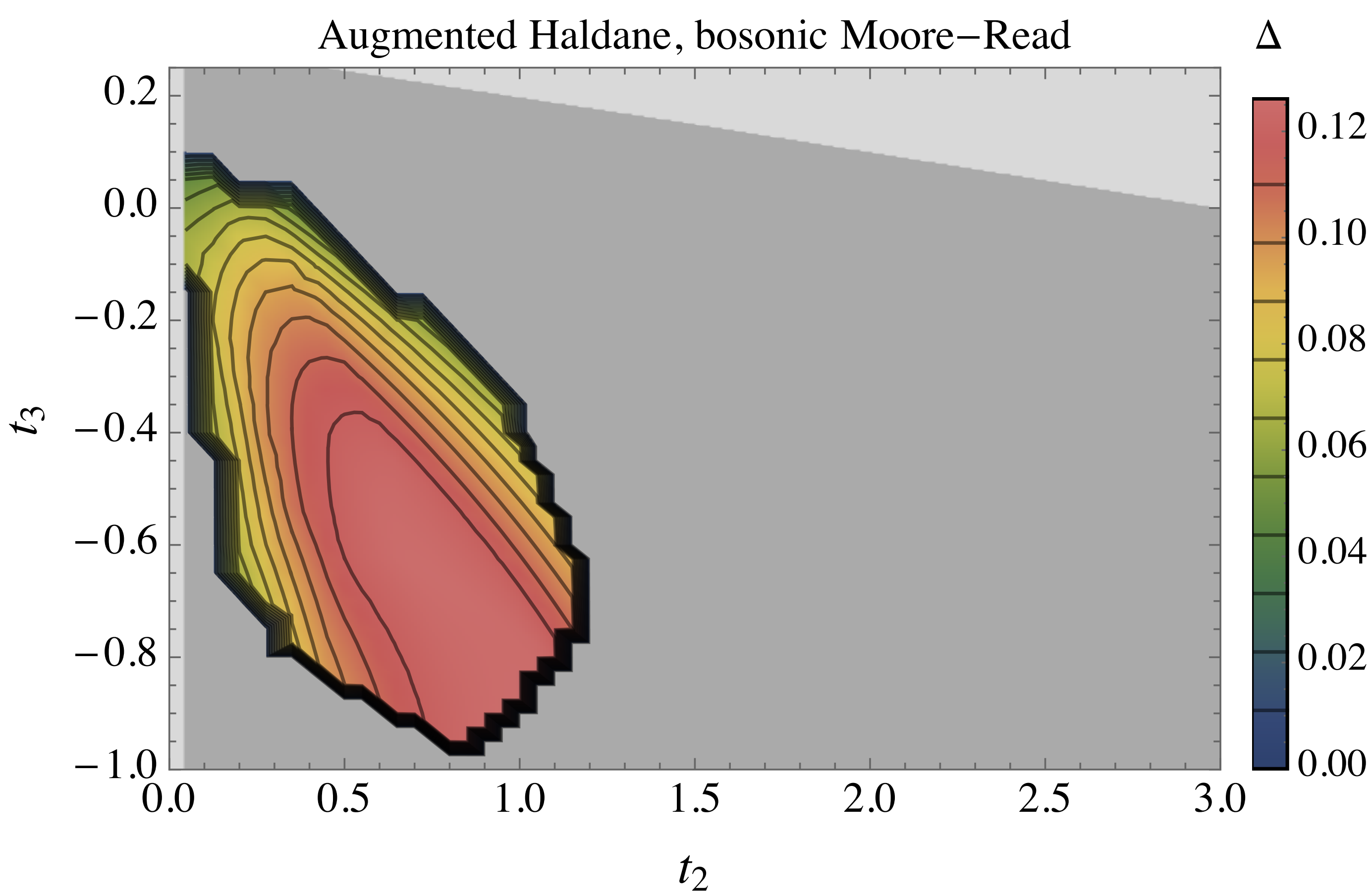

Short-distance physics in FQHE

Most well-known approach: trial wavefunction formalism

Laughlin ‘83: Account for Coulomb repulsion by extra Jastrow factors (cf. superfluid ^{4}He)

$$\Psi_L(z_1, \ldots, z_N) \propto \boxed{\prod_{i<j} (z_i - z_j)^m} \cdot e^{-\frac{1}{4}\sum_i |z_i|^2} \qquad \nu = \frac{1}{m}$$

(validated by exact diagonalization)

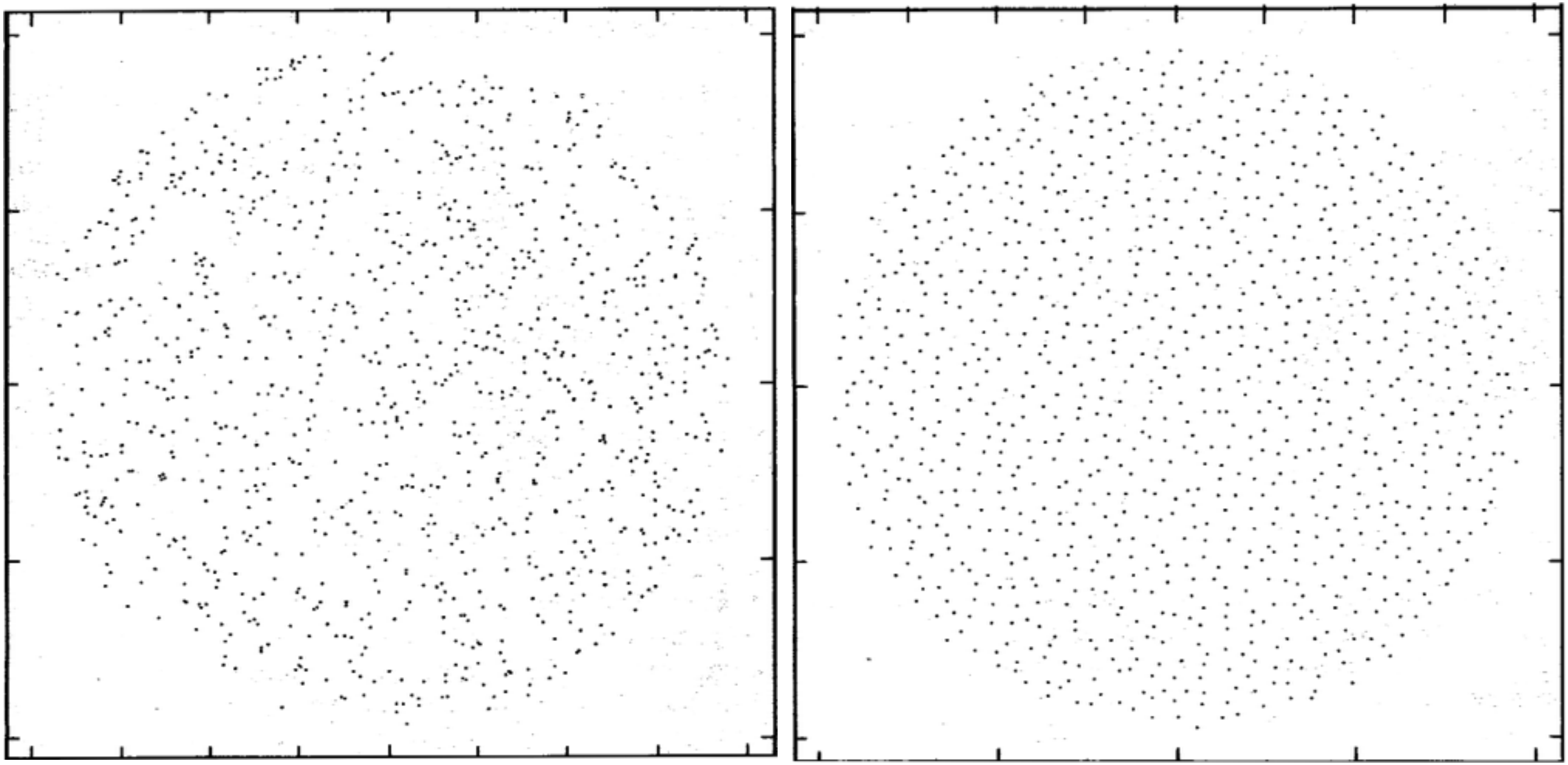

From R. B. Laughlin in ***The quantum Hall effect****, eds. R. E. Prange and S. M. Girvin (1987)*

Comparison of a random distribution of electrons (left) with a “typical” one for electrons described by the Laughlin wavefunction. The configuration on the right is more probable by a factor of 10^{6080}.

Short-distance physics in FQHE

$$\Psi_L(z_1, \ldots, z_N) \propto \prod_{i<j} (z_i - z_j)^m \cdot e^{-\frac{1}{4}\sum_i |z_i|^2} \qquad \nu = \frac{1}{m}$$

Trial wavefunctions rely on the analytic structure inherent to the LLL; their success is based on keeping electrons far from each other.

Proposals have been made for porting these to lattice FCIs, but this essential feature gets lost in the process. Thus, we are led to search for alternative formulations of the problem.

Review of the SMA

- Feynman-Bijl theory of ^{4}He:

> “Rather than look at the Hamiltonian we shall ‘wave our hands,’ use analogies with simpler systems, draw pictures, and make plausible guesses based on physical intuition to obtain a qualitative picture of the solutions (wave functions).”
>
> — R. P. Feynman, *Statistical Mechanics* (1972)

Review of the SMA

- Feynman-Bijl theory of ^{4}He:
  - Bose statistics → GS is real, positive, nodeless, symmetric. Maximal amplitude on configurations with evenly spaced particles.
  - A change in density can't be obtained through permutations of atoms. → Bose statistics don't affect phonon states.

Review of the SMA

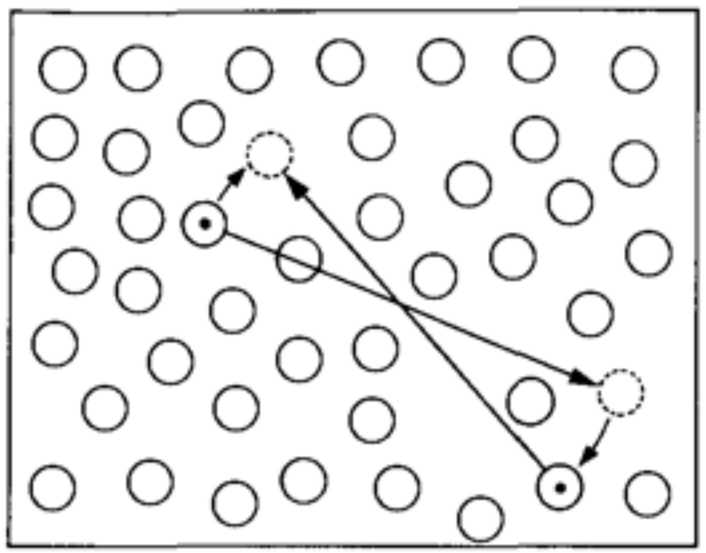

Two configurations (solid and dotted) that result from large displacements (long arrows) of the atoms, can actually be accomplished by much smaller adjustments (short arrows) due to the bosonic statistics of the atoms. Figure reproduced from R. P. Feynman, *Statistical Physics* (1972).

- Argue by contradiction that any low-energy non-phonon excitation must have an amplitude that's negative for at least some configurations of particles with uniform density (in order to be orthogonal to GS and phonons.) But, because of Bose statistics, all these configurations must be *equivalent*.

Review of the SMA

- Low-energy excitations are all long-wavelength phonons.

$$|\psi\rangle_{\text{phonon, small }\mathbf{k}} = \sum_i e^{i\mathbf{k}.\mathbf{r}_i}|\phi\rangle$$

- Higher-energy excitations must involve density fluctuations over shorter length scales, of the form $|\psi\rangle = \sum_i f(\mathbf{r}_i)|\phi\rangle$.

  Using a variational argument, can show energy is optimized for $f(\mathbf{r}_i) = e^{i\mathbf{k}.\mathbf{r}_i}$.

    - For **k** of order 1/a, these are rotons.

GMP

- Naive application of SMA to QHE at v=1:

  Structure factor $s(k) = 1 - \exp(-k^2 l^2/2)$,

  thus $\Delta(k) = \dfrac{\hbar^2 k^2}{2m[1 - \exp(-k^2 l^2/2)]}$,

  but, noting that $\hbar^2/ml^2 = \hbar\omega_c$,

  we obtain $\Delta(k) = \hbar\omega_c \dfrac{(kl)^2}{1 - \exp(-k^2 l^2/2)}$

  as required by Kohn's theorem.

- GMP: for fractional v, must have same k→0 limit, by Kohn's theorem. Implies naive SMA variational states will have most amplitude in higher LLs.

Kohn's theorem : In the limit of zero wave vector, the cyclotron mode occurs at precisely $\hbar\omega_c$ and saturates the oscillator strength sum rule for the exact (interacting) ground state.

- GMP idea: obtain more physical variational excitations for FQHE by projecting $\rho_{\mathbf{k}}|\phi\rangle$ to LLL.

- Physical interpretation of the roton minimum in FQHE: precursor of instability to Wigner crystallization.

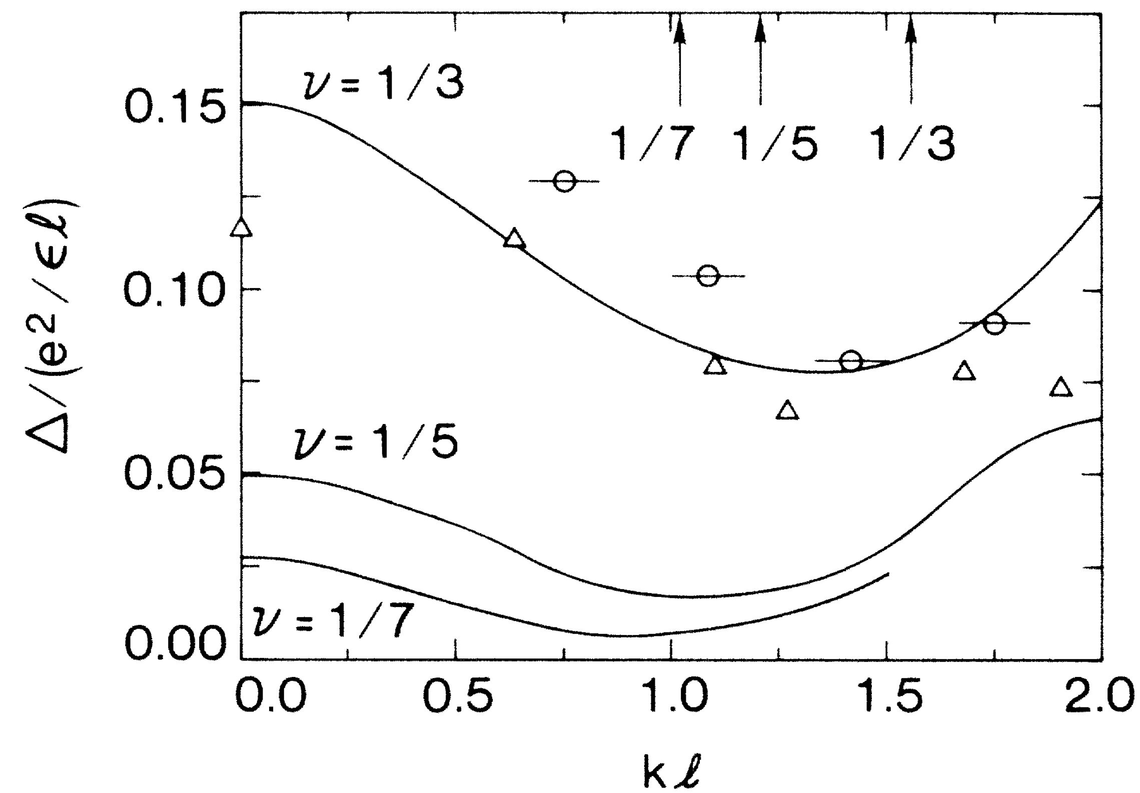

FIG. 4. Comparison of SMA prediction of collective mode energy for $\nu=\frac{1}{3}, \frac{1}{5}, \frac{1}{7}$ with numerical results of Haldane and Rezayi (Ref. 20) for $\nu=\frac{1}{3}$. Circles are from a seven-particle spherical system. Horizontal error bars indicate the uncertainty in converting angular momentum on the sphere to linear momentum. Triangles are from a six-particle system with a hexagonal unit cell. Arrows have same meaning as in Fig. 3.

GMP algebra (w/LLL form factor):

$$[\rho_{\mathrm{LLL}}(\mathbf{q}),\rho_{\mathrm{LLL}}(\mathbf{q}')] =$$
$$2i\sin\left(\tfrac{1}{2}\mathbf{q}\wedge\mathbf{q}'\ell_B^2\right)\exp\left(\tfrac{1}{2}\mathbf{q}\cdot\mathbf{q}'\ell_B^2\right)\rho_{\mathrm{LLL}}(\mathbf{q}+\mathbf{q}')$$

Use this to express f($\mathbf{q}$) in terms of s($\mathbf{q}$),
so gap only depends on s($\mathbf{q}$):

$$\bar{f}(\mathbf{k}) = \frac{1}{2}\sum_{\mathbf{q}} v(\mathbf{q})(e^{q^*k/2-qk^*/2})\times$$
$$[\bar{s}(\mathbf{q})e^{-k^2/2}(e^{-k^*q/2}-e^{-kq^*/2})+\bar{s}(\mathbf{k}+\mathbf{q})(e^{k^*q/2}-e^{kq^*/2})]$$

Our approach

- “Reasonable assumption”: LLL is the optimal flat Chern band for FQH phenomena.
- Distance of any Chern band to LLL can then be used as a measure of suitability for FQH-like physics.

Motivation

R. Roy, PRB **90**, 165139 (2014).
S. A. Parameswaran, R. Roy and S. L. Sondhi, C. R. Physique **14**, 816 (2013)

- How do we define distance between non-isomorphic Hilbert spaces?
- Reasonable to assume that the essential physics of LLL is captured by GMP commutation relations.
- It is plausible that, if the GMP algebra is obeyed by a projected Chern band, the SMA approximation will also hold.
- **Strategy**: for Chern band, look at how closely algebra of projected density operators approximates GMP algebra.

Our approach

$$\overline{\rho}_{\mathbf{q}} \equiv \mathcal{P}_\alpha \rho(\mathbf{q}) \mathcal{P}_\alpha = \sum_{\mathbf{k}} \left(\sum_b u_b^{\alpha *}\left(\mathbf{k}+\frac{\mathbf{q}}{2}\right) u_b^{\alpha}\left(\mathbf{k}-\frac{\mathbf{q}}{2}\right) \right)$$

$$\gamma^\dagger_{\mathbf{k}+\frac{\mathbf{q}}{2},\alpha} \gamma_{\mathbf{k}-\frac{\mathbf{q}}{2},\alpha}$$

At long wavelengths $qa \ll 1$ we may expand

$$\sum_b u_b^{\alpha *}\left(\mathbf{k}+\frac{\mathbf{q}}{2}\right) u_b^{\alpha}\left(\mathbf{k}-\frac{\mathbf{q}}{2}\right) \approx 1 - i\mathbf{q}\cdot \sum_b u_b^{\alpha *}(\mathbf{k}) \frac{\nabla_{\mathbf{k}}}{i} u_b^{\alpha}(\mathbf{k})$$

$$\approx e^{i\int_{\mathbf{k}-\mathbf{q}/2}^{\mathbf{k}+\mathbf{q}/2} d\mathbf{k}'\cdot \mathcal{A}_\alpha(\mathbf{k}')}$$

Our approach

$$\left[\overline{\rho}_{\mathbf{q}_1}, \overline{\rho}_{\mathbf{q}_2}\right] \approx i\,\mathbf{q}_1 \wedge \mathbf{q}_2 \sum_{\mathbf{k}} \Bigg[\mathcal{B}_\alpha(\mathbf{k}) \sum_b u_b^{\alpha *}(\mathbf{k}_+)\, u_b^{\alpha}(\mathbf{k}_-) \\ \times \gamma^\dagger_{\mathbf{k}_+,\alpha}\gamma_{\mathbf{k}_-,\alpha}\Bigg]$$

Assume Berry curvature is constant: $\overline{\mathcal{B}}_\alpha = \dfrac{\int_{\mathrm{BZ}} d\mathbf{k}\, \mathcal{B}_\alpha(\mathbf{k})}{\int_{\mathrm{BZ}} d\mathbf{k}} = \dfrac{2\pi C_\alpha}{A_{\mathrm{BZ}}}$

Then $[\overline{\rho}_{\mathbf{q}_1}, \overline{\rho}_{\mathbf{q}_2}] \approx i\mathbf{q}_1 \wedge \mathbf{q}_2 \overline{\mathcal{B}}_\alpha \overline{\rho}_{\mathbf{q}_1+\mathbf{q}_2}$

Our approach

Expand GMP order-by-order around $\mathbf{q} \sim 0.$ Closure?

O($\mathbf{q}^2$): Berry curvature constant over BZ.

O($\mathbf{q}^3$): Pullback of HS metric constant over BZ.

$$ds^2 = \langle\delta\psi|\delta\psi\rangle - \langle\delta\psi|\psi\rangle\langle\psi|\delta\psi\rangle$$

$$g_{\mu\nu} + \tfrac{i}{2}F_{\mu\nu}$$
$$= \sum_{\alpha\in\mathrm{occ}} \mathrm{tr}\, \left(\tfrac{\partial}{\partial k_\mu}P_\alpha\right)(1-P_\alpha)\left(\tfrac{\partial}{\partial k_\nu}P_\alpha\right)$$

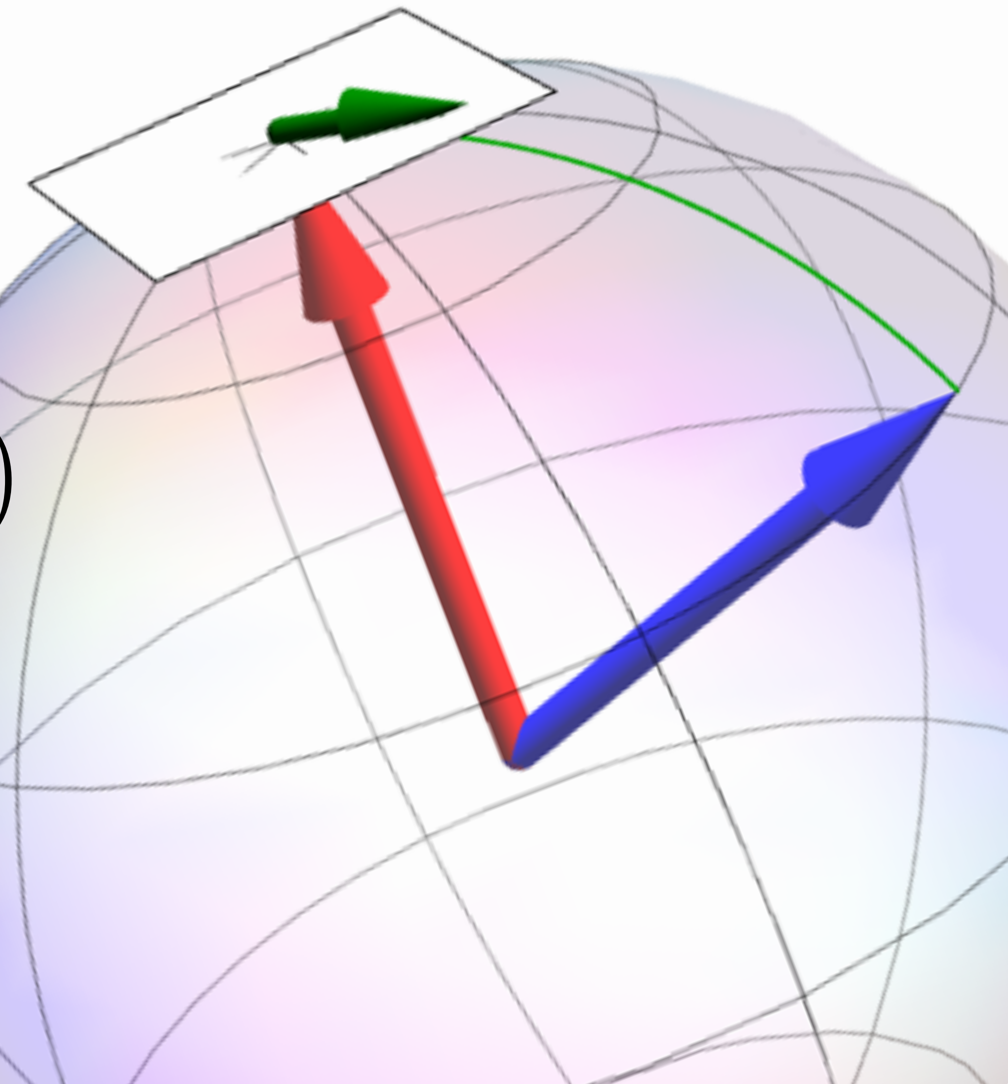

Our approach

Expand GMP order-by-order around $\mathbf{q} \sim 0.$ Closure?

O($\mathbf{q}^2$): Berry curvature constant over BZ.

O($\mathbf{q}^3$): Pullback of HS metric constant over BZ.

Can show $\mathrm{tr}\; g_{\mu\nu}(\mathbf{k}) \geq |B(\mathbf{k})| \quad \Rightarrow \det g \geq \frac{1}{4}|B|^2$

Saturating metric trace inequality is **stricter** than determinant inequality: means projected density operators **identical** to GMP algebra, not merely isomorphic.

Our approach

Expand GMP order-by-order around $\mathbf{q} \sim 0.$ Closure?

O($\mathbf{q}^2$): Berry curvature constant over BZ.

O($\mathbf{q}^3$): Pullback of HS metric constant over BZ.

Closure at ***all* higher orders** if $\det g = \frac{1}{4}|B|^2$

$$[\overline{\rho}_{\mathbf{q}_1}, \overline{\rho}_{\mathbf{q}_2}] = 2i \sin\left(\frac{\mathbf{q}_1 \wedge \mathbf{q}_2 \overline{B}_\alpha}{2}\right) e^{q_{1,\ell}\overline{g}^{\alpha}_{\ell m} q_{2,m}} \overline{\rho}_{\mathbf{q}_1+\mathbf{q}_2}$$

- Both Berry curvature and FS metric appear in this form of the GMP algebra. Algebra applies to higher Chern number bands as well.
- Conditions for “good bands” can be stated purely in terms of the FS metric alone.

Results: Haldane model

F. D. M. Haldane, Phys. Rev. Lett. **61**, 2015 (1988).

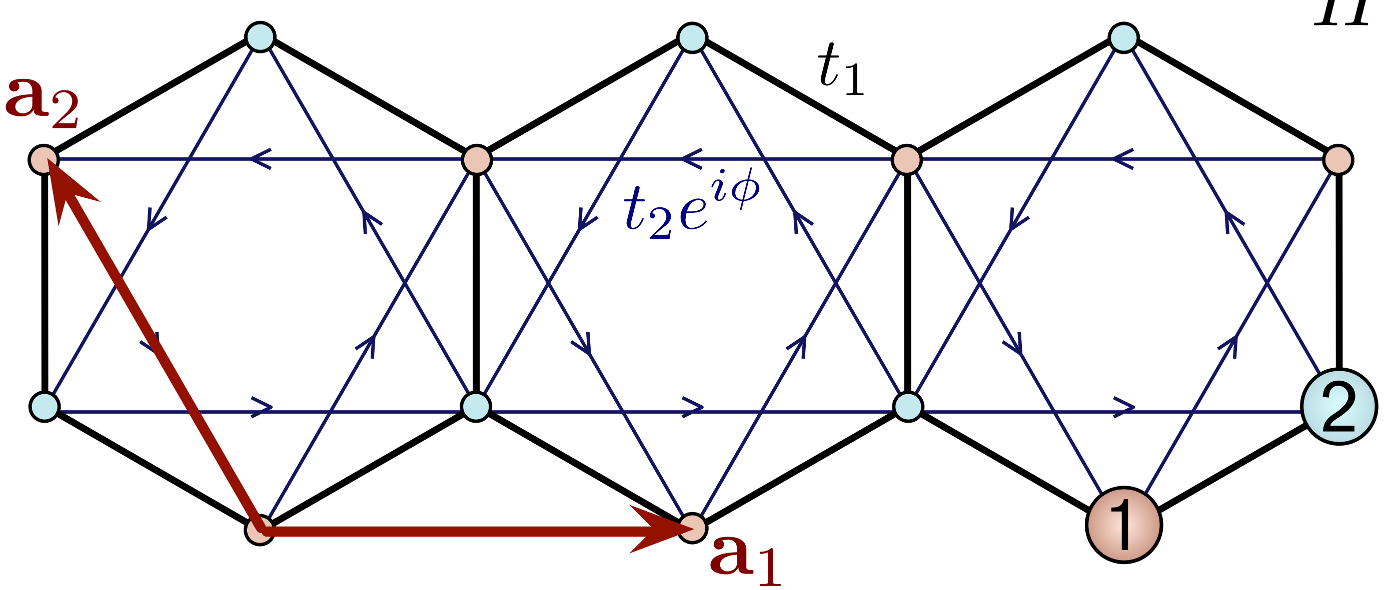

$$H = \sum_{NN} t_1 \sigma_X \cos k \cdot \mathbf{a_i} + t_1 \sigma_Y \sum_{NN} \sin k \cdot \mathbf{a_i} + \sigma_Z \left(\mu_{AB} - 2t_2 \sin \phi \sum_{NNN} \sin k \cdot \mathbf{a'_i} \right)$$

Gap vs. geometry

(a)- gaps for bosonic Laughlin, (b)- gaps for fermionic Laughlin, (c) & (d)- plots along M=0

- Location of max gap for bosonic and fermionic Laughlin agrees with min RMS B
- Band geometry “interpolates” between bosonic, fermionic statistics
- For this model, quantum metric does not provide info beyond that supplied by curvature.

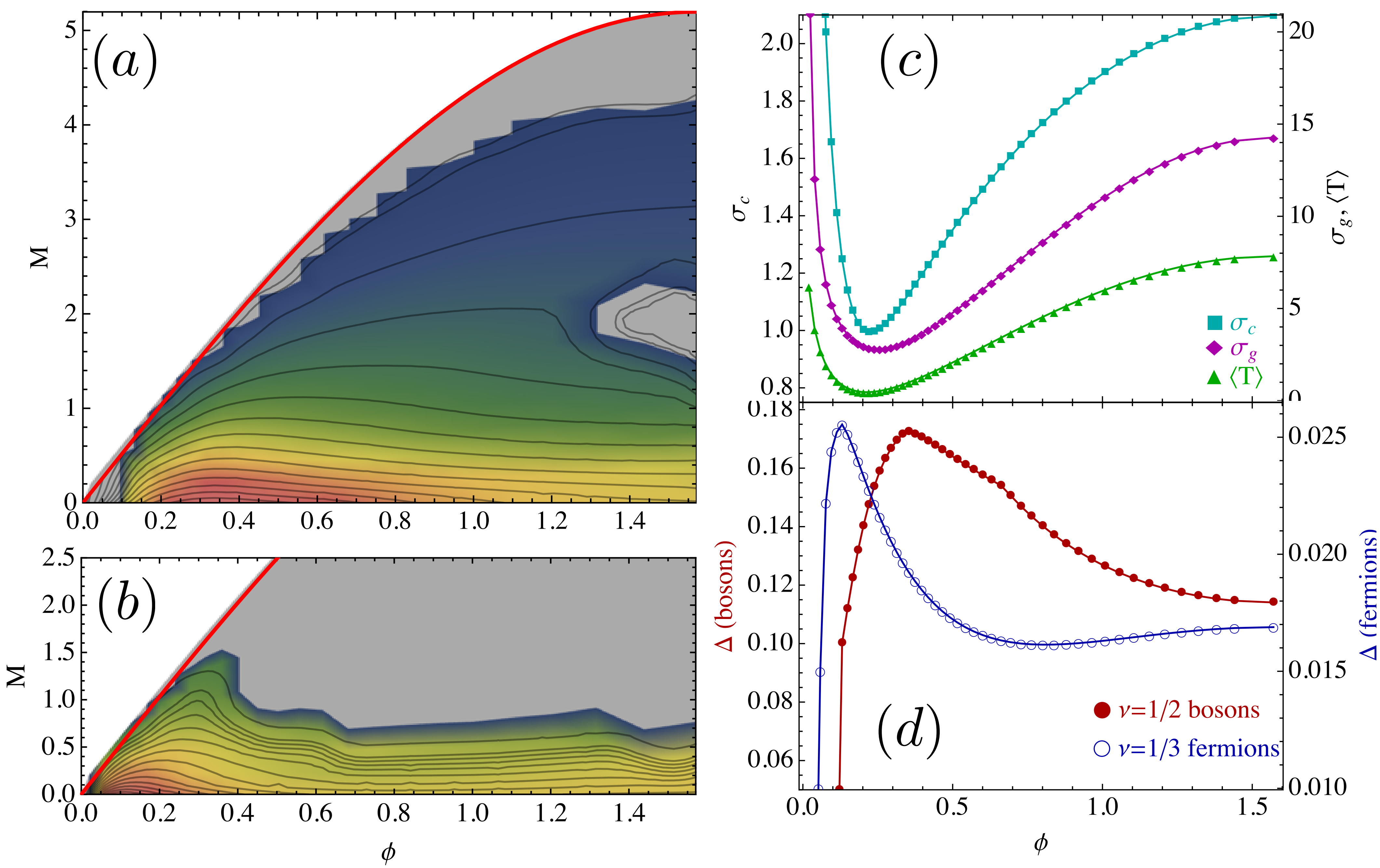

Augmented Haldane model

- Add additional third-NN hopping to Haldane Hamiltonian
- Set mass M=0; space of remaining relevant couplings still 2d
- Motivation: 1) reduce curvature fluctuations to level seen in Kagome, ruby 2) Enlarge space of couplings in order to investigate effects of quantum metric.

Geometry & gap for new parameterization of Haldane-t3

- Now have large range of parameters with uniform curvature
- Minimum trace inequality in distinct location from min RMS B

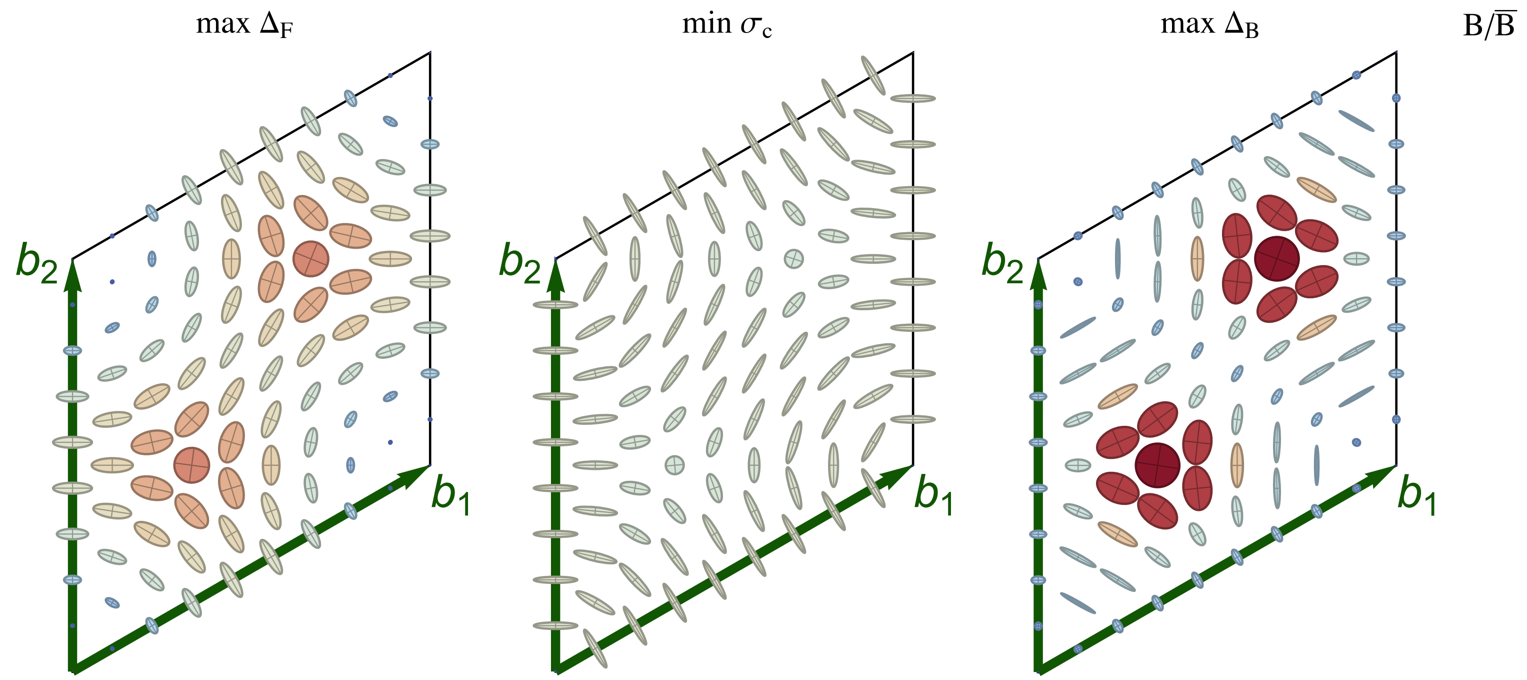

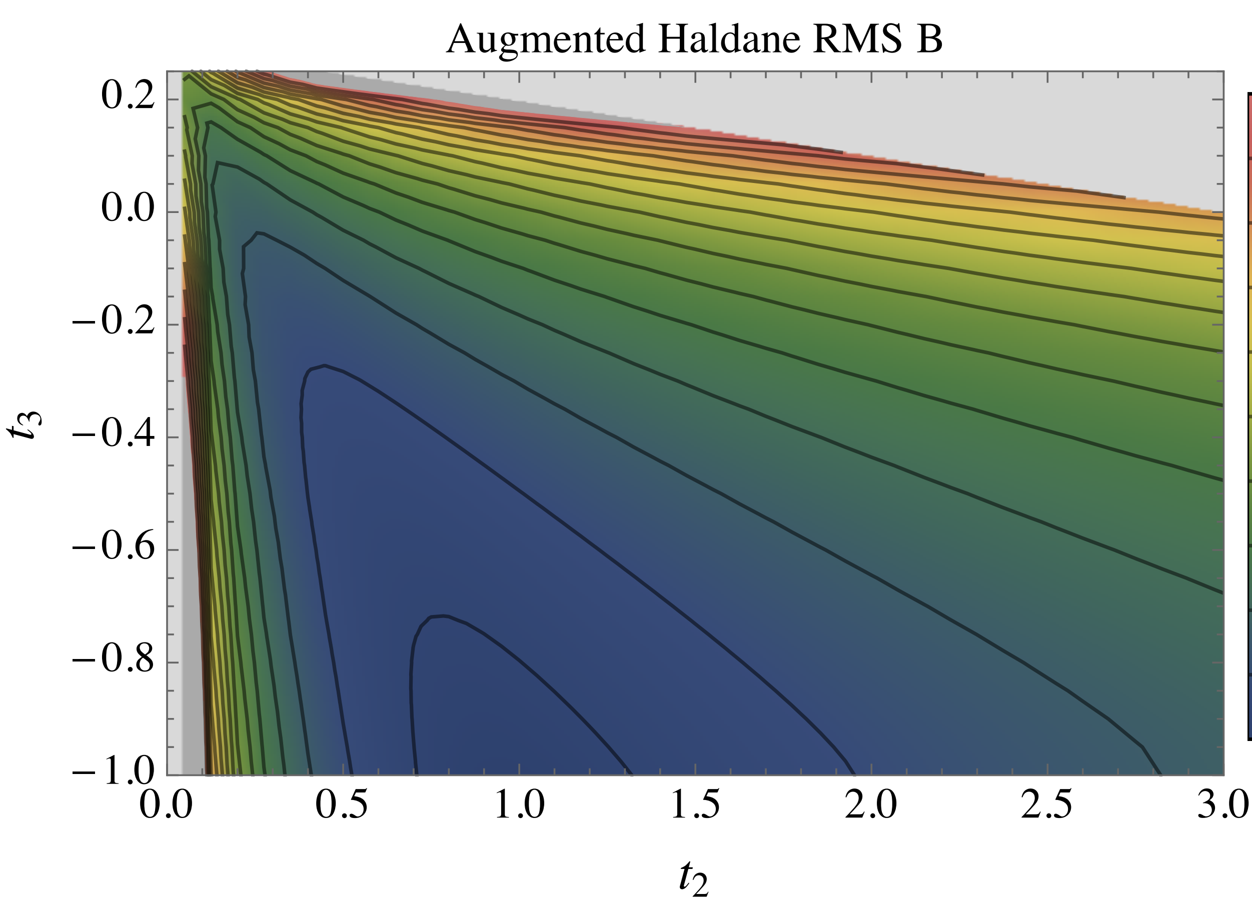

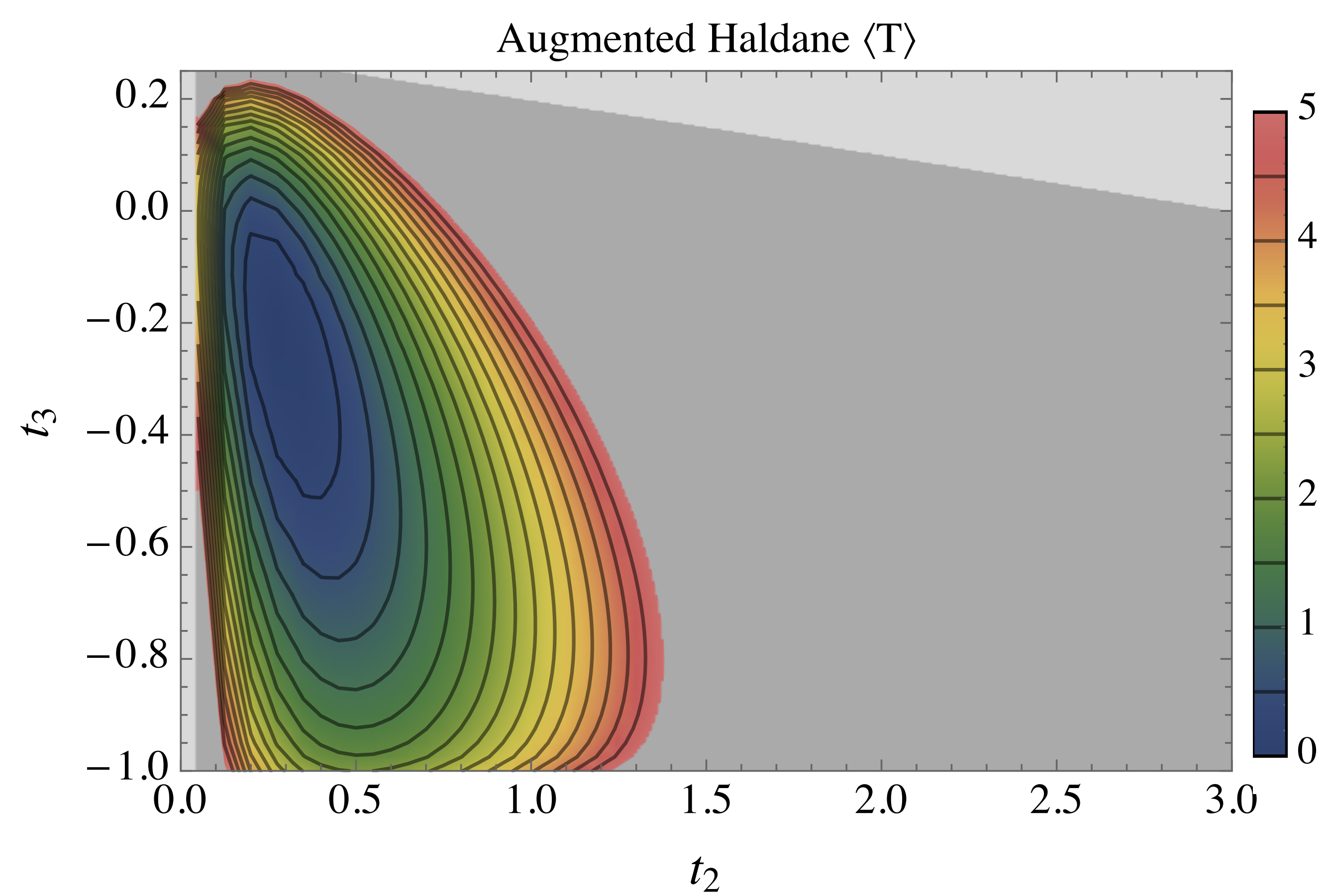

Geometry & gap for new parameterization of Haldane-t3

- Interpret leftward shift of max gap position in bosonic Laughlin state as being due to influence of metric trace inequality (also seen in fermionic Laughlin)

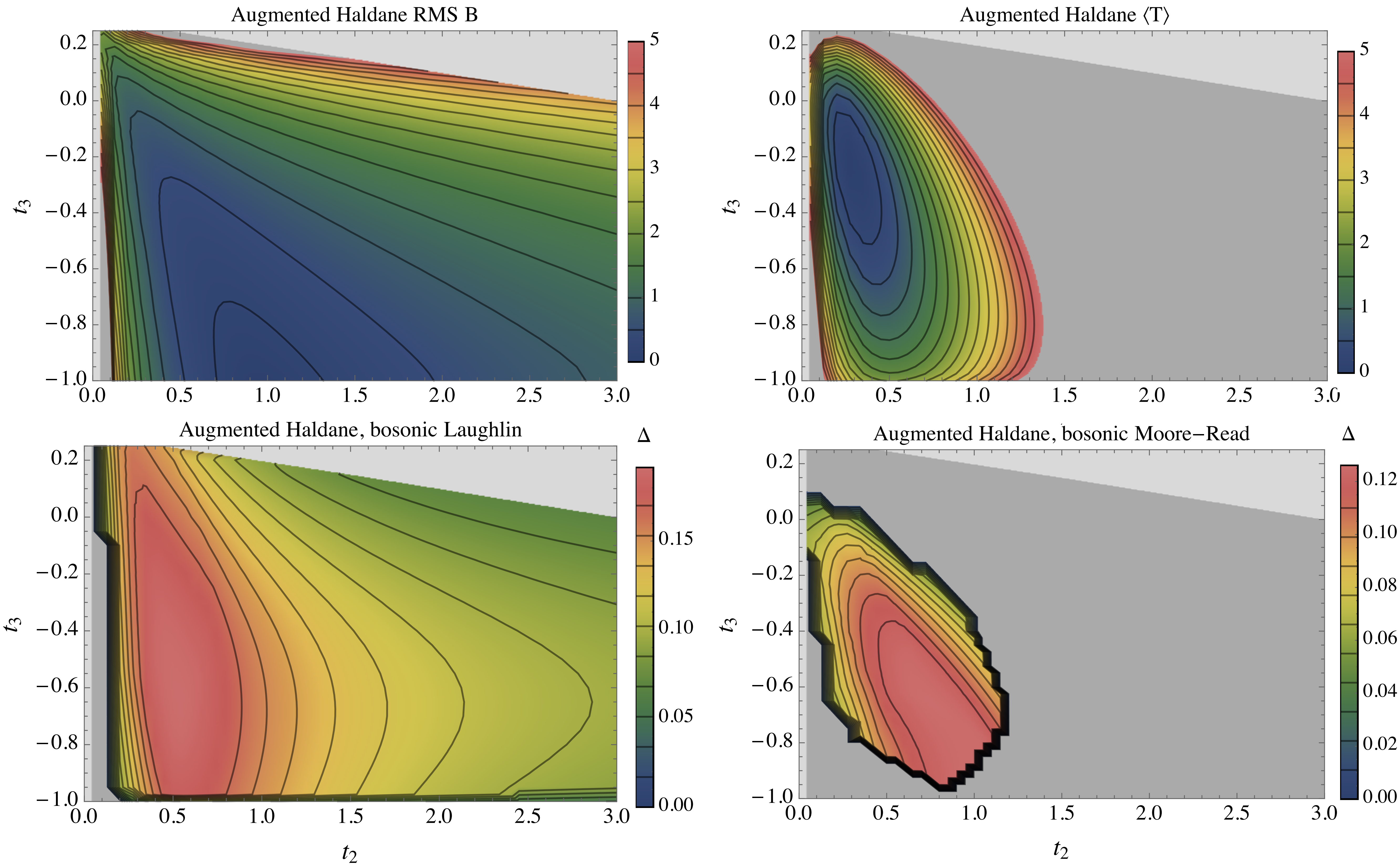

Results: Kagome lattice model

Tang, Mei and Wen, PRL **106**, 236802 (2011)

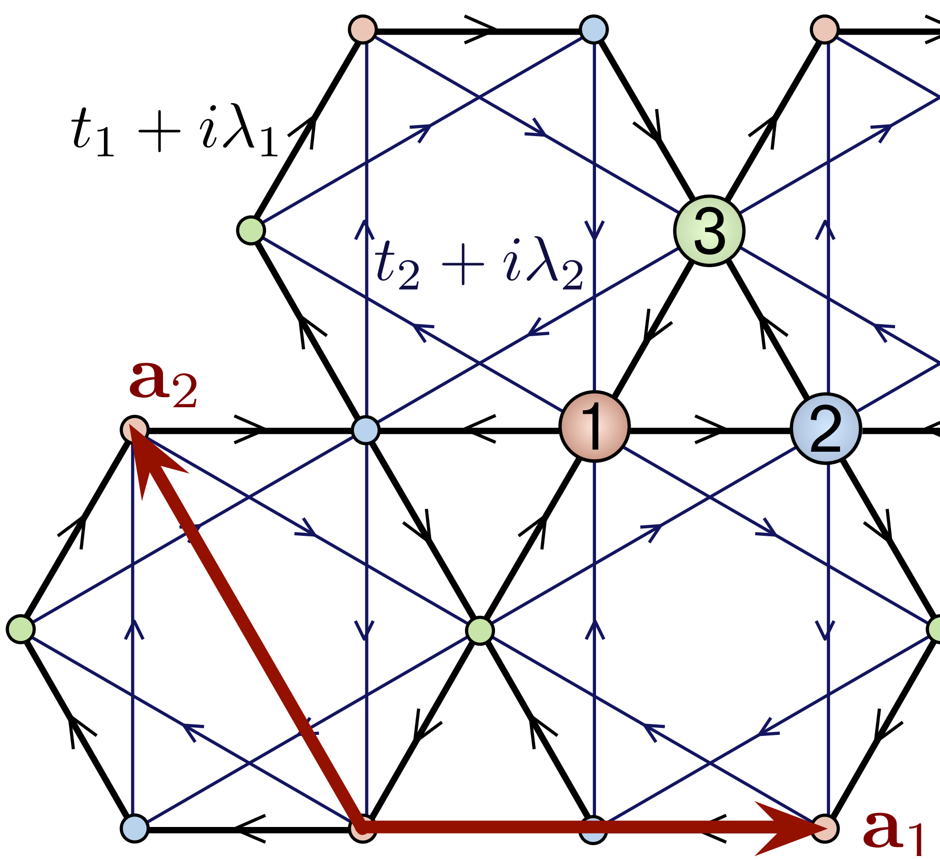

$$
\begin{aligned}
H = -2t_1 &\begin{pmatrix} 0 & \cos k_1 & \cos k_2 \\ & 0 & \cos k_3 \\ \mathrm{hc} & & 0 \end{pmatrix} \\
+ 2i\lambda_1 &\begin{pmatrix} 0 & \cos k_1 & -\cos k_2 \\ & 0 & \cos k_3 \\ -\mathrm{hc} & & 0 \end{pmatrix} \\
- 2t_2 &\begin{pmatrix} 0 & \cos k_2 + k_3 & \cos k_3 - k_1 \\ & 0 & \cos k_1 + k_2 \\ \mathrm{hc} & & 0 \end{pmatrix} \\
+ 2i\lambda_2 &\begin{pmatrix} 0 & -\cos k_2 + k_3 & \cos k_3 - k_1 \\ & 0 & -\cos k_1 + k_2 \\ -\mathrm{hc} & & 0 \end{pmatrix}
\end{aligned}
$$

Gap vs. RMS B and Tr G for NN-only Kagome model

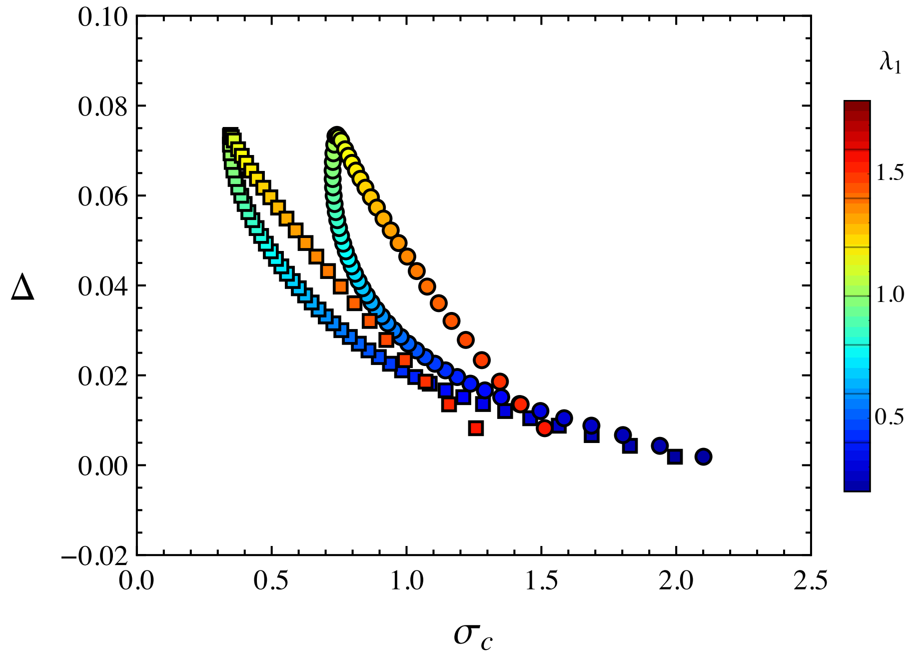

- Looking at (correct) RMS B alone shows two branches
- Branches distinguished by including information about metric trace inequality
- Pattern holds in both bosonic Laughlin and bosonic Moore-Read states

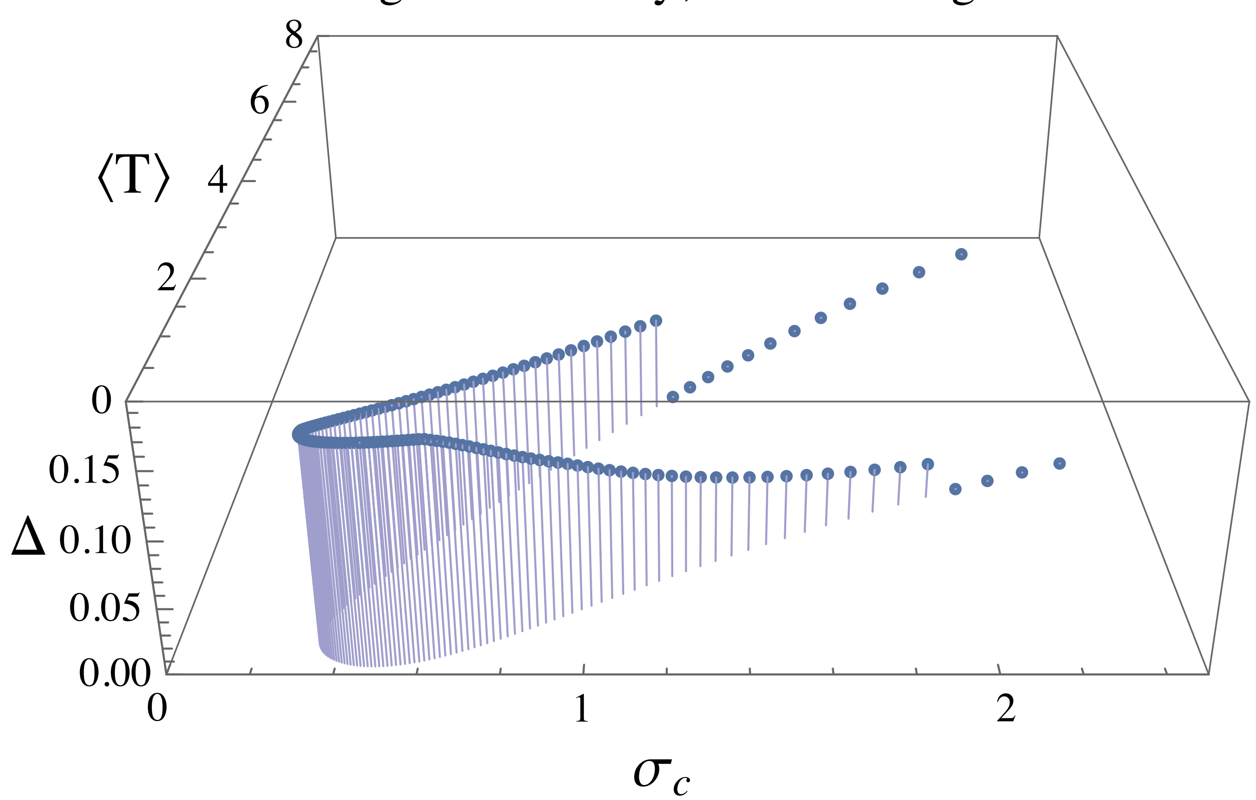

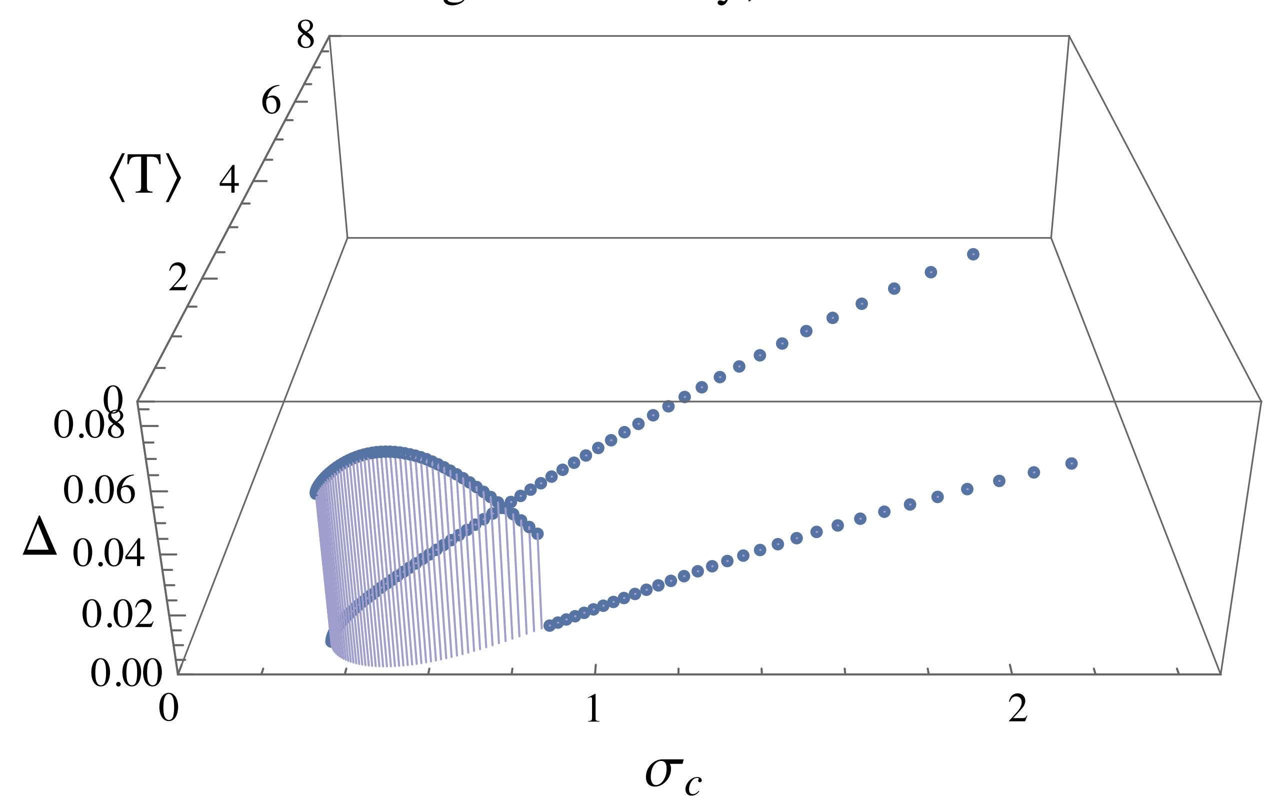

Gap vs RMS B, Kagome model, bosonic Laughlin

- Approximately linear trend which holds from min RMS B point all the way to the phase boundary (gap closure)
- Significant scatter, though, which may be explained by quantum metric

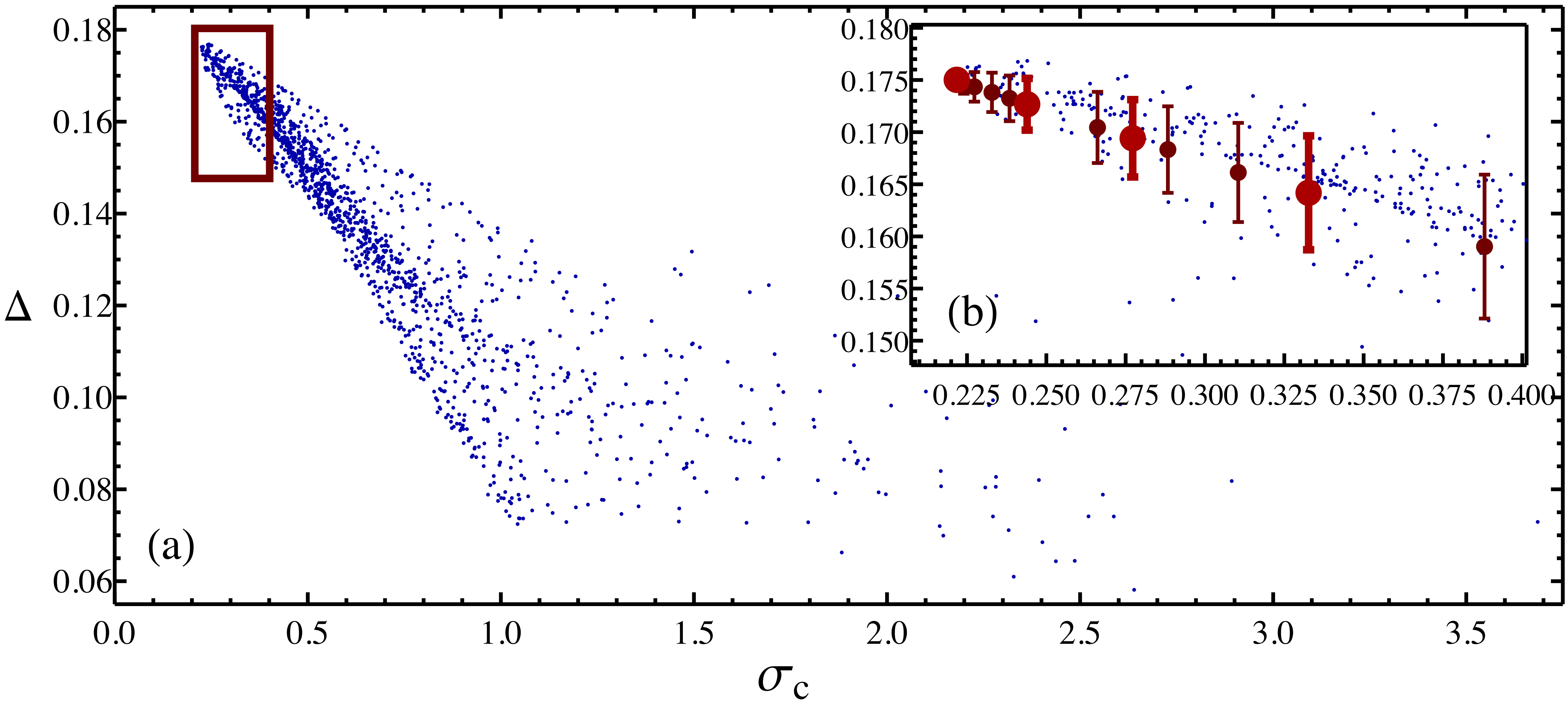

Shells of constant RMS B

- Including all points with low RMS B yields a clear one-way trend, in the sense that the largest gaps are obtained only for parameters with low ⟨T ⟩
- Sampling points in parameter space from isosurfaces of constant RMS B shows linear correlation between gap and metric trace

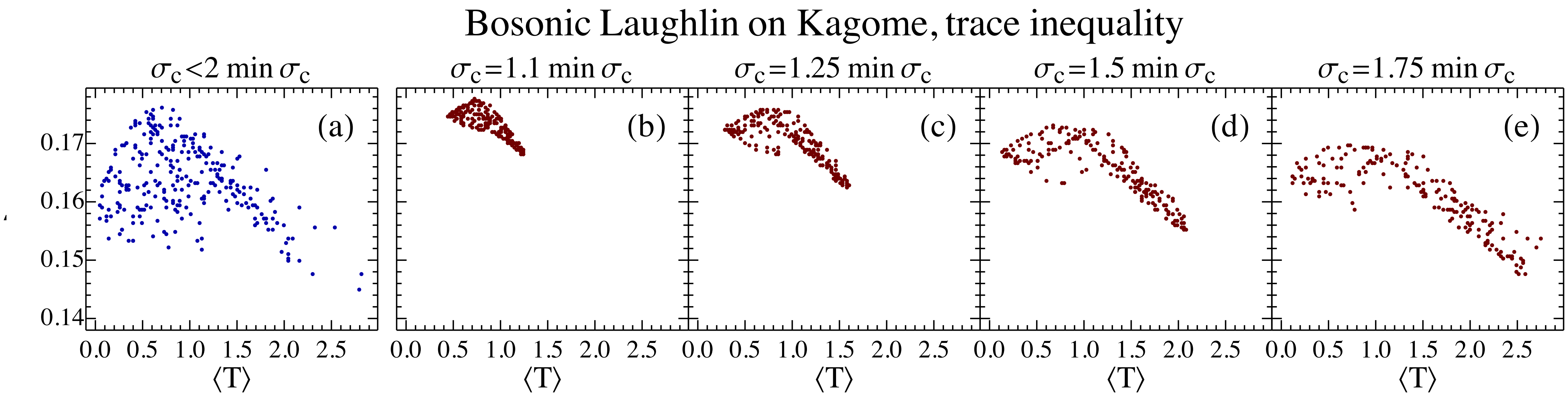

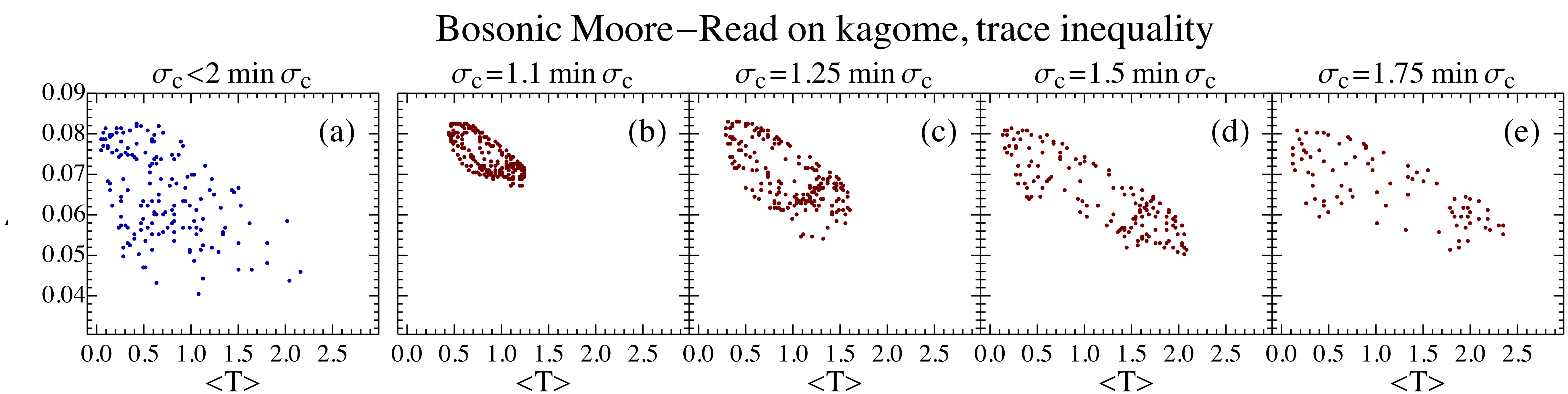

Results: Ruby lattice model

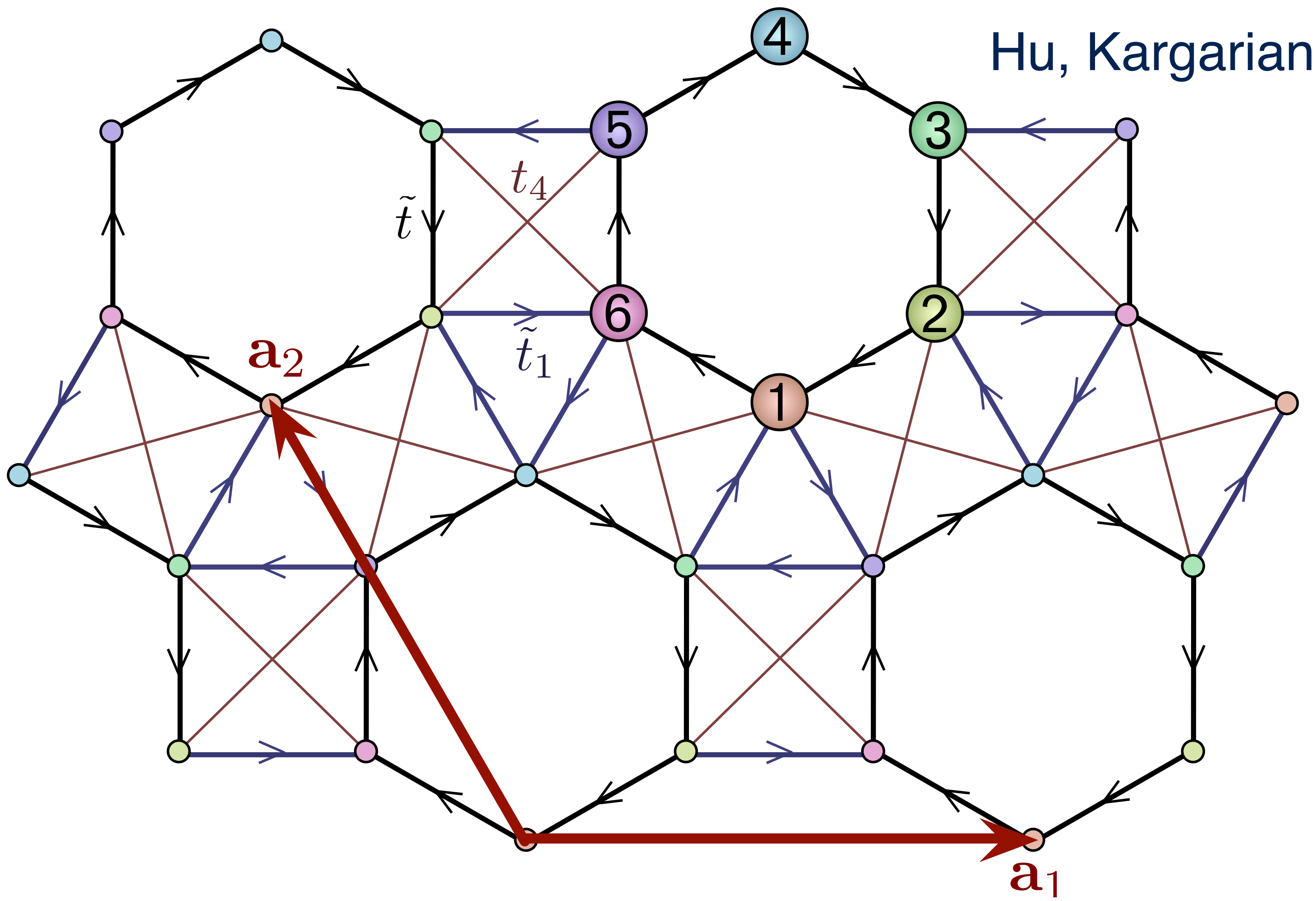

Hu, Kargarian and Fiete, PRB **84**, 155116 (2011)

Gap vs RMS B, ruby model, bosonic Laughlin

- Similar linear dependence of gap on RMS B as seen in Kagome model

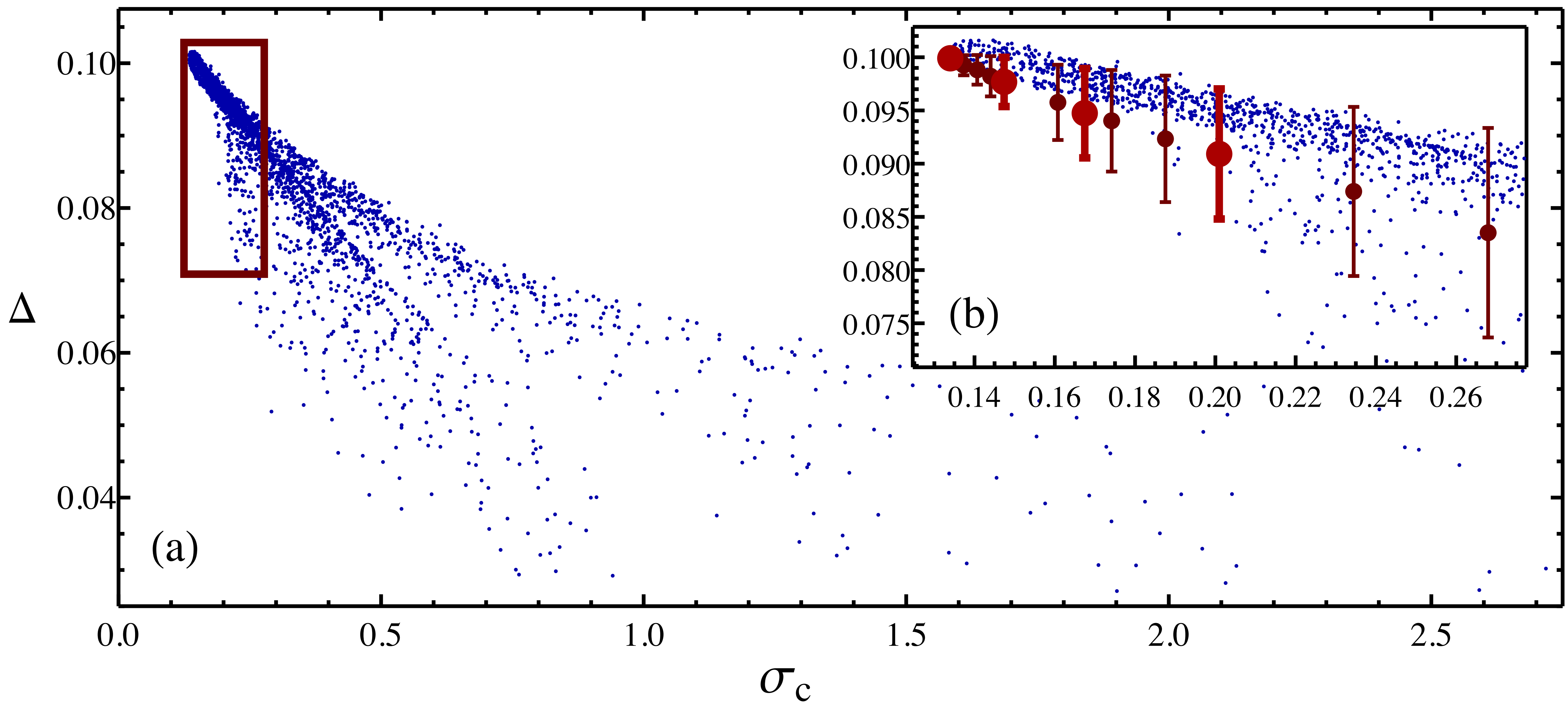

Shells of constant RMS B

- Including all points with low RMS B yields a clear one-way trend, in the sense that the largest gaps are obtained only for parameters with low ⟨T ⟩
- Sampling points in parameter space from isosurfaces of constant RMS B shows linear correlation between gap and metric trace

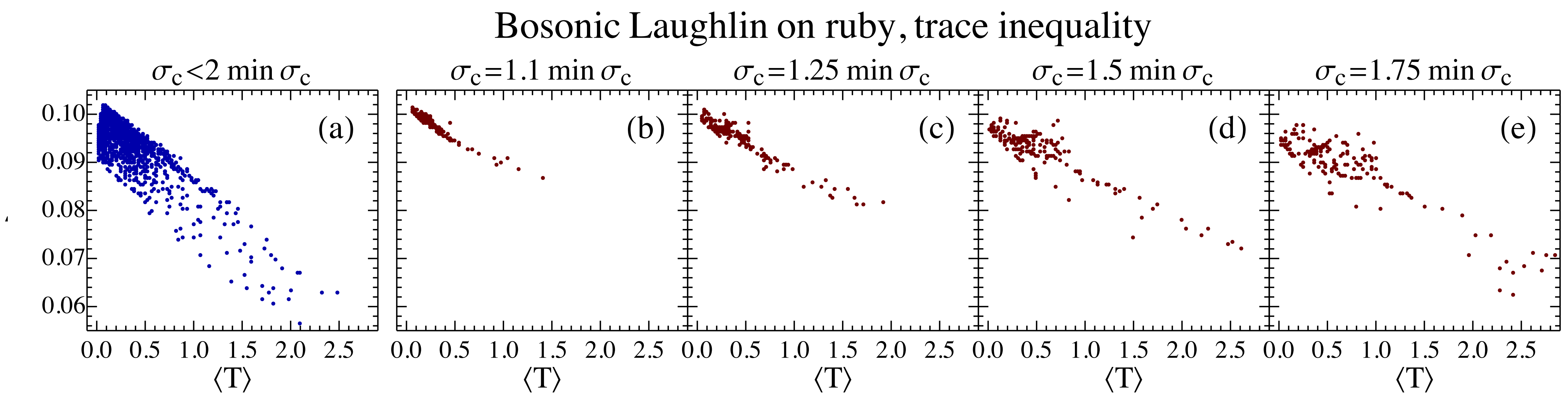

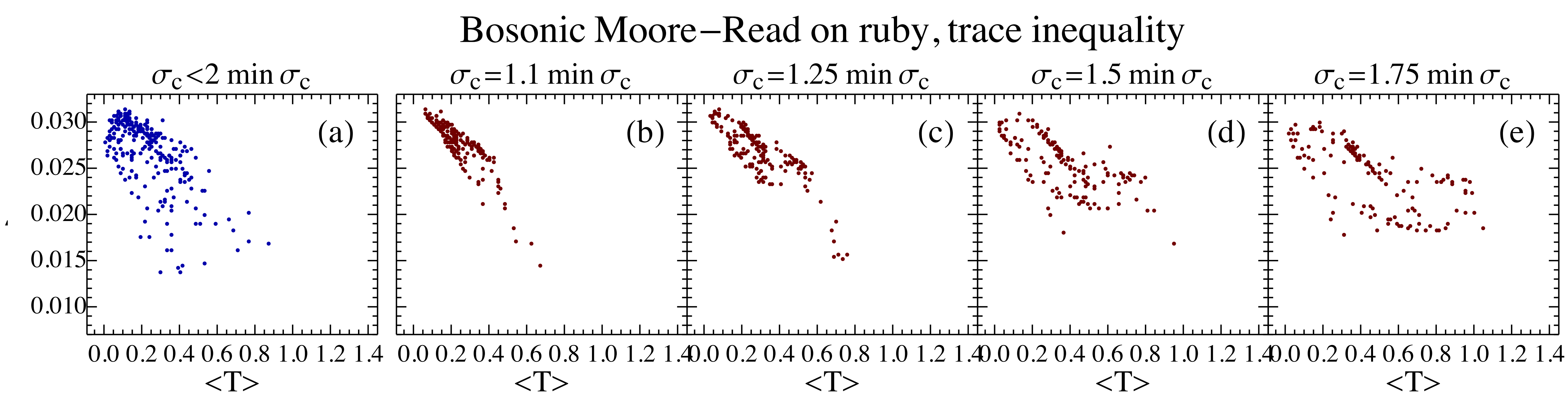

Weak data collapse

Red, green, blue are ruby, kagome and Haldane-t3

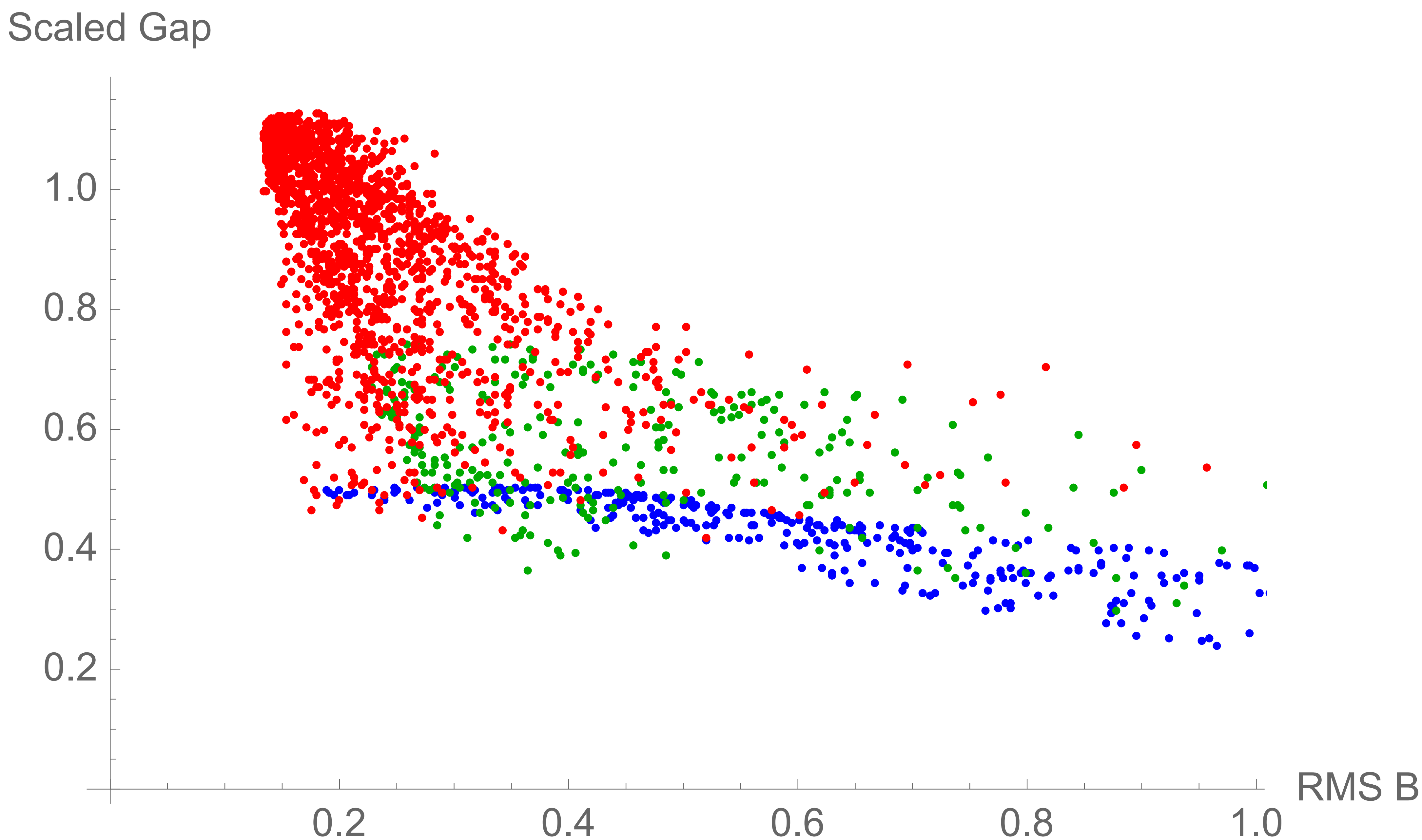

Topological order and space group symmetries

- Topological order in the FQHE and in the Chern bands arises at fractional fillings
- Theorems due to Oshikawa and Hastings extending previous work of Lieb, Schultz and Mattis tell us that at fractional fillings, without spontaneous symmetry breaking, a gap can arise only in conjunction with topological order
- We can now show that even at certain integer fillings of systems with nonsymmorphic space group symmetries, without spontaneous symmetry breaking, a gap can only arise in conjunction with topological order [RR, 2012, Parameswaran et al, 2012]

Nonsymmorphic symmetry of diamond

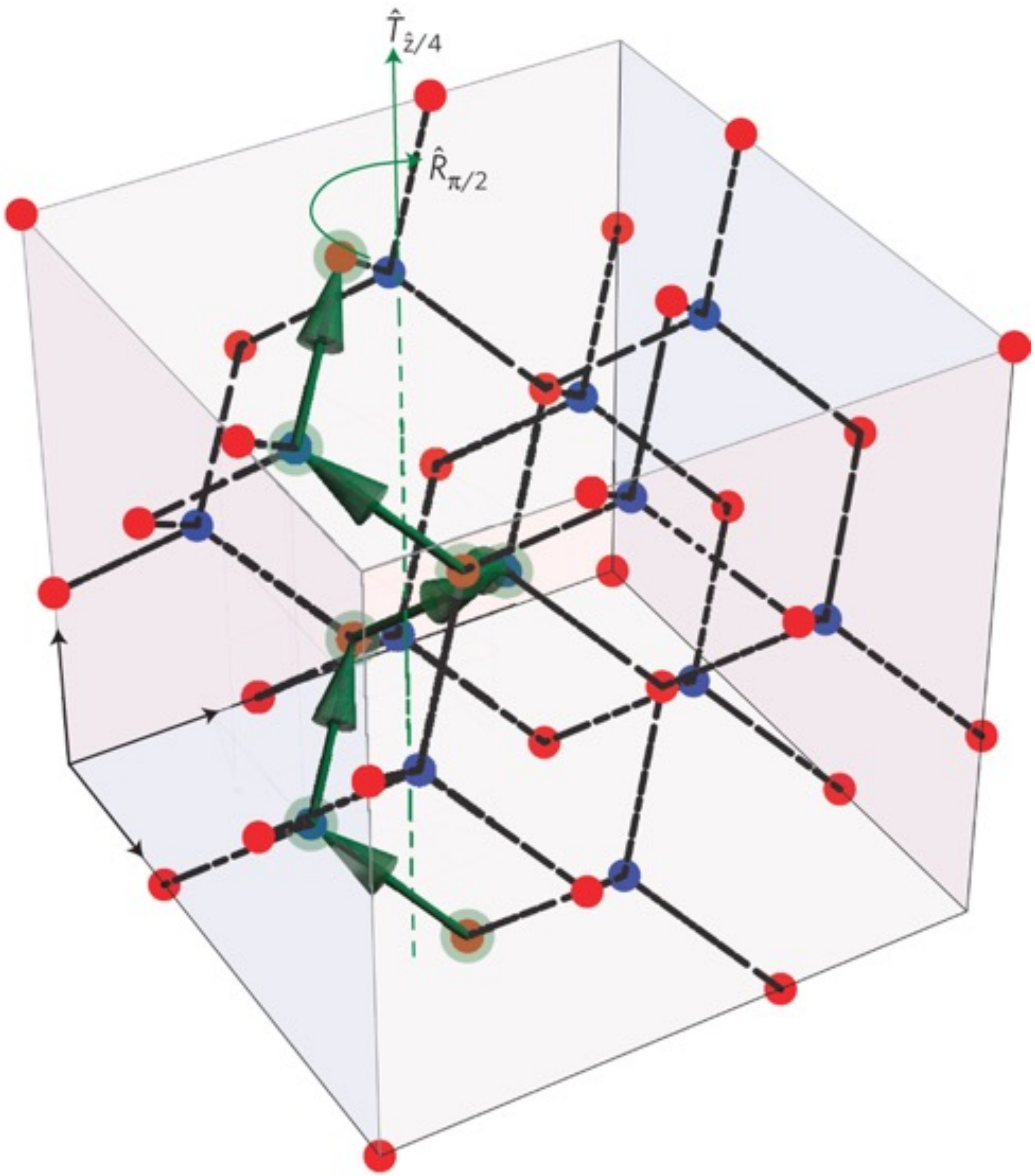

[from Parameswaran et al]

End

Cross-model comparisons

Quantifying degree of correlation on shells of const. RMS B — Spearman ρ monotonicity test

- Nonparametric statistic which is sensitive to any monotonic relationship
- Perfect correlation for ρ = ±1, no correlation at ρ = 0
- Find siginifcant, robust negative correlation between gap and metric inequality on all isosurfaces of constant RMS B, demonstrating importance of trace inequality as a subleading influence on the gap

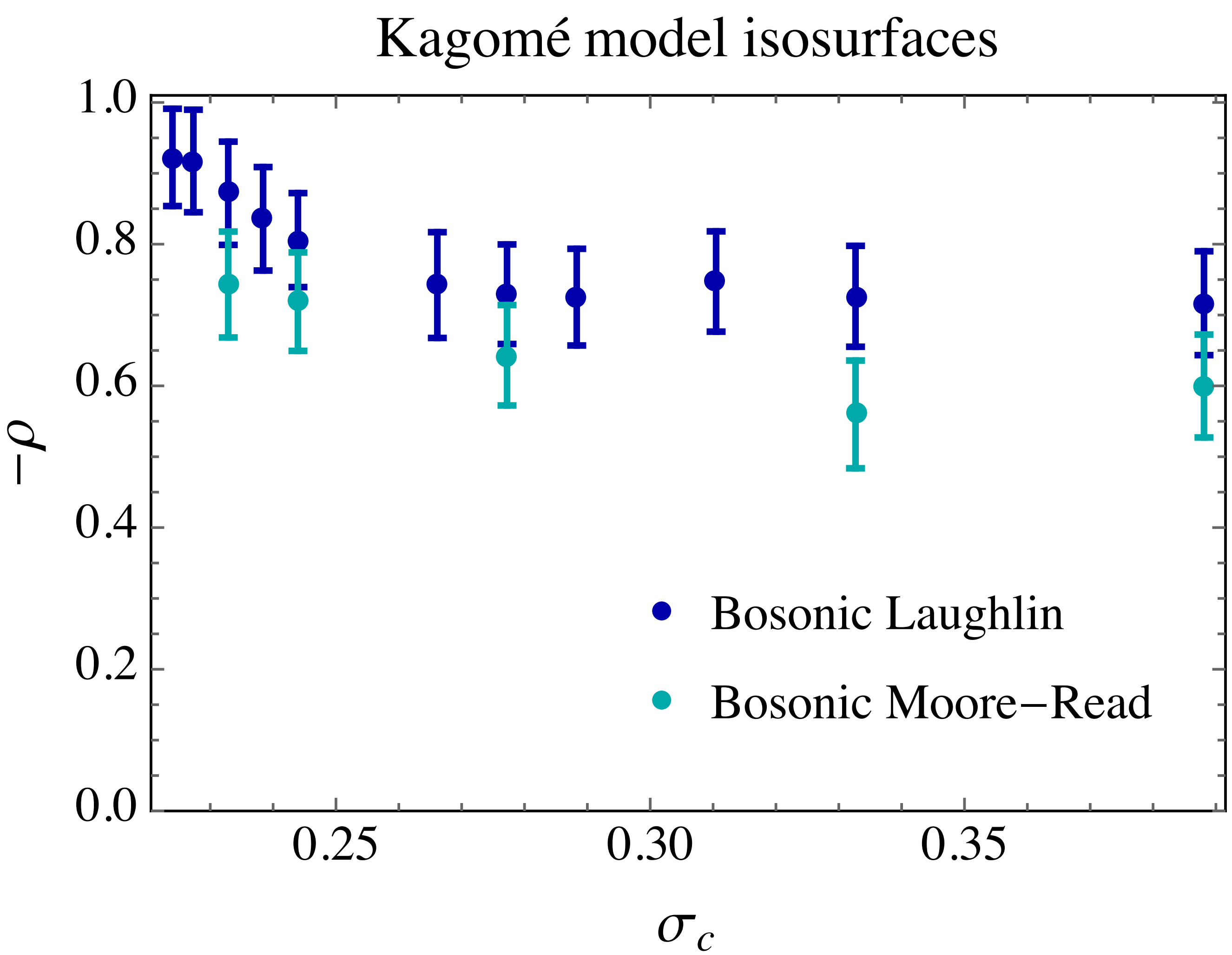

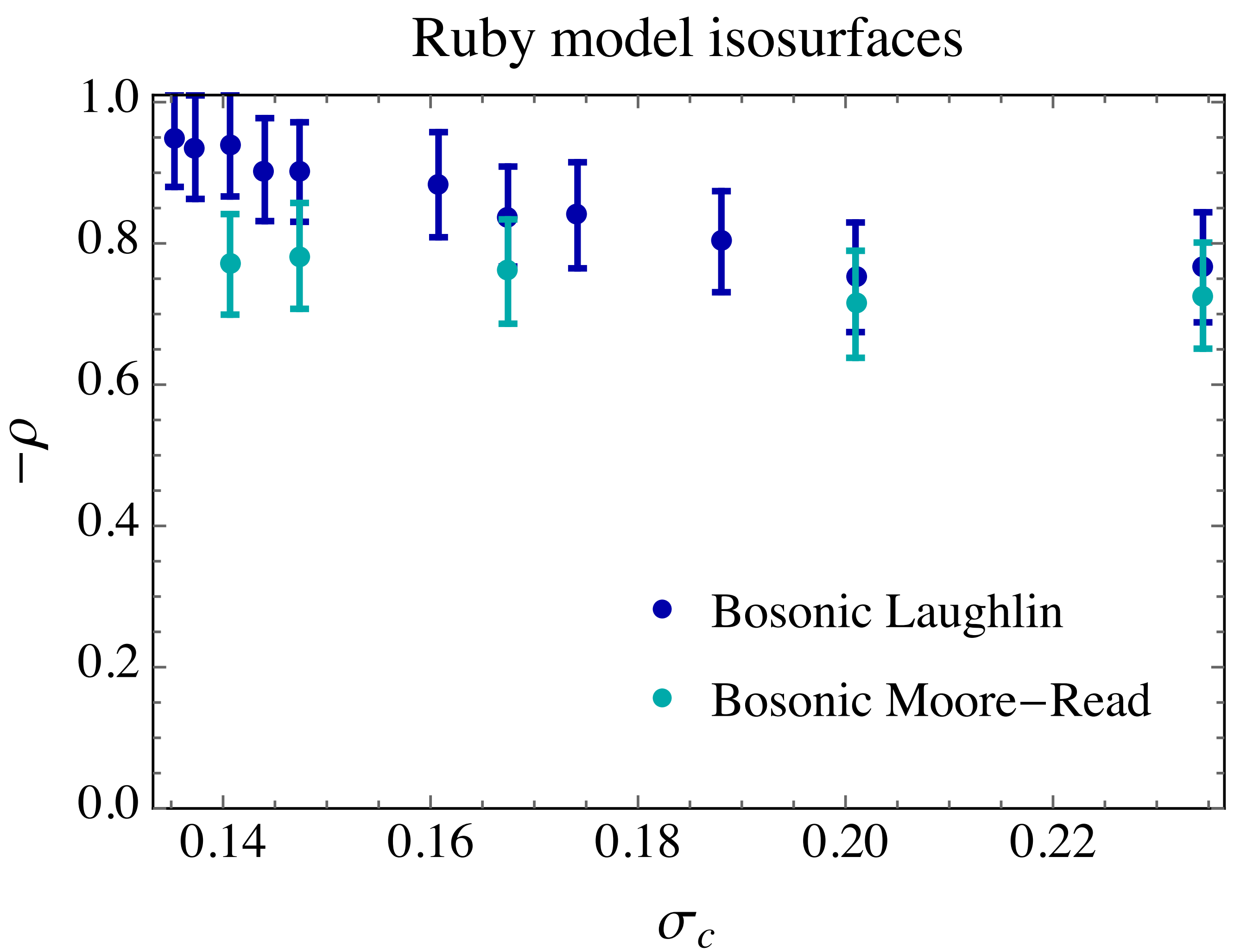

Gaps vs. RMS B and trace inequality

- Parameters yielding max gap are always in lower-left corner
- Demonstrates relevance of both band-geometric quantities

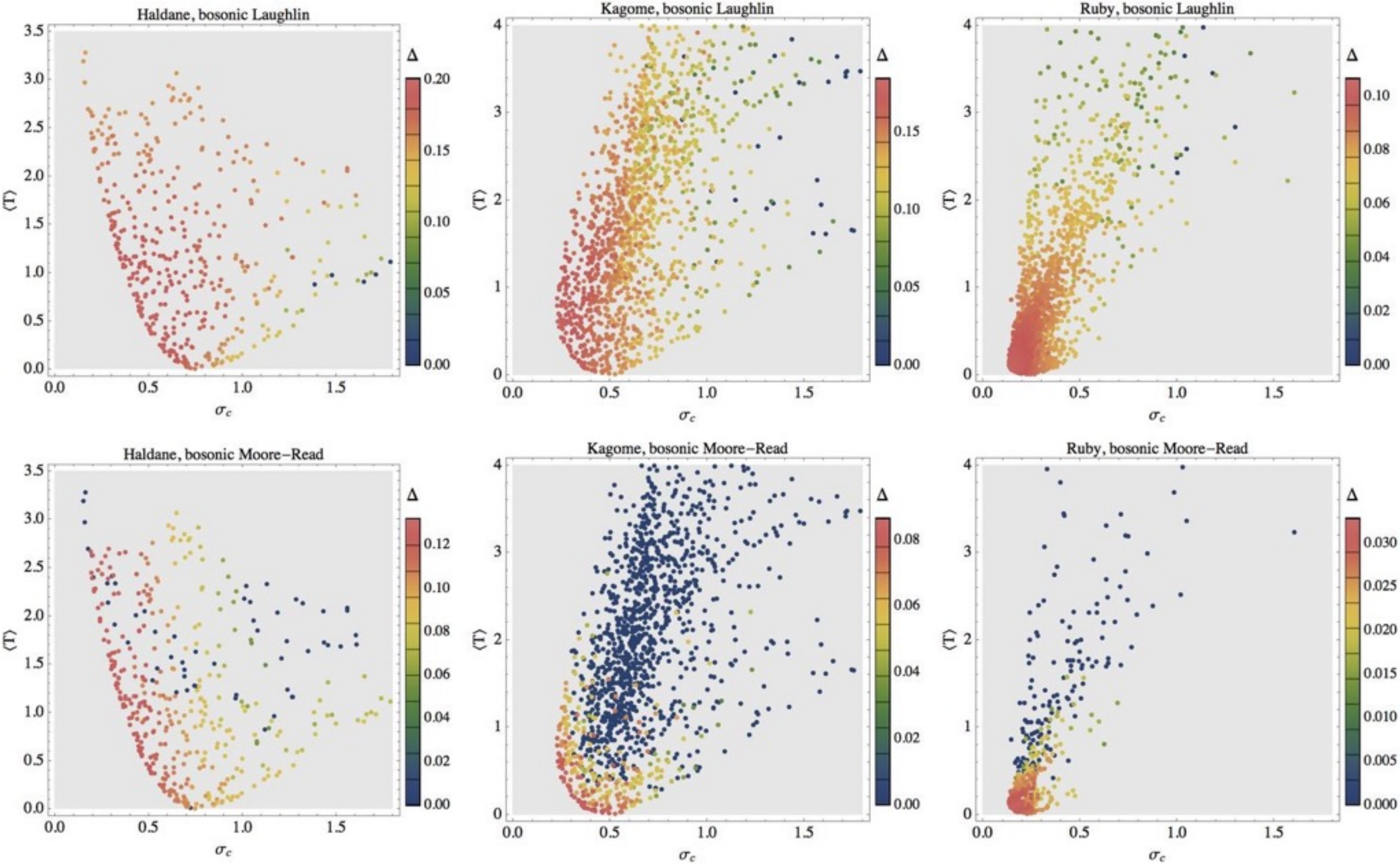

Scaled gaps vs. RMS B and trace inequality

- Scaling argument: *k*-particle δ-fn interaction means gap should scale as N^(k-1)
- Polygon = region of common support of all three models

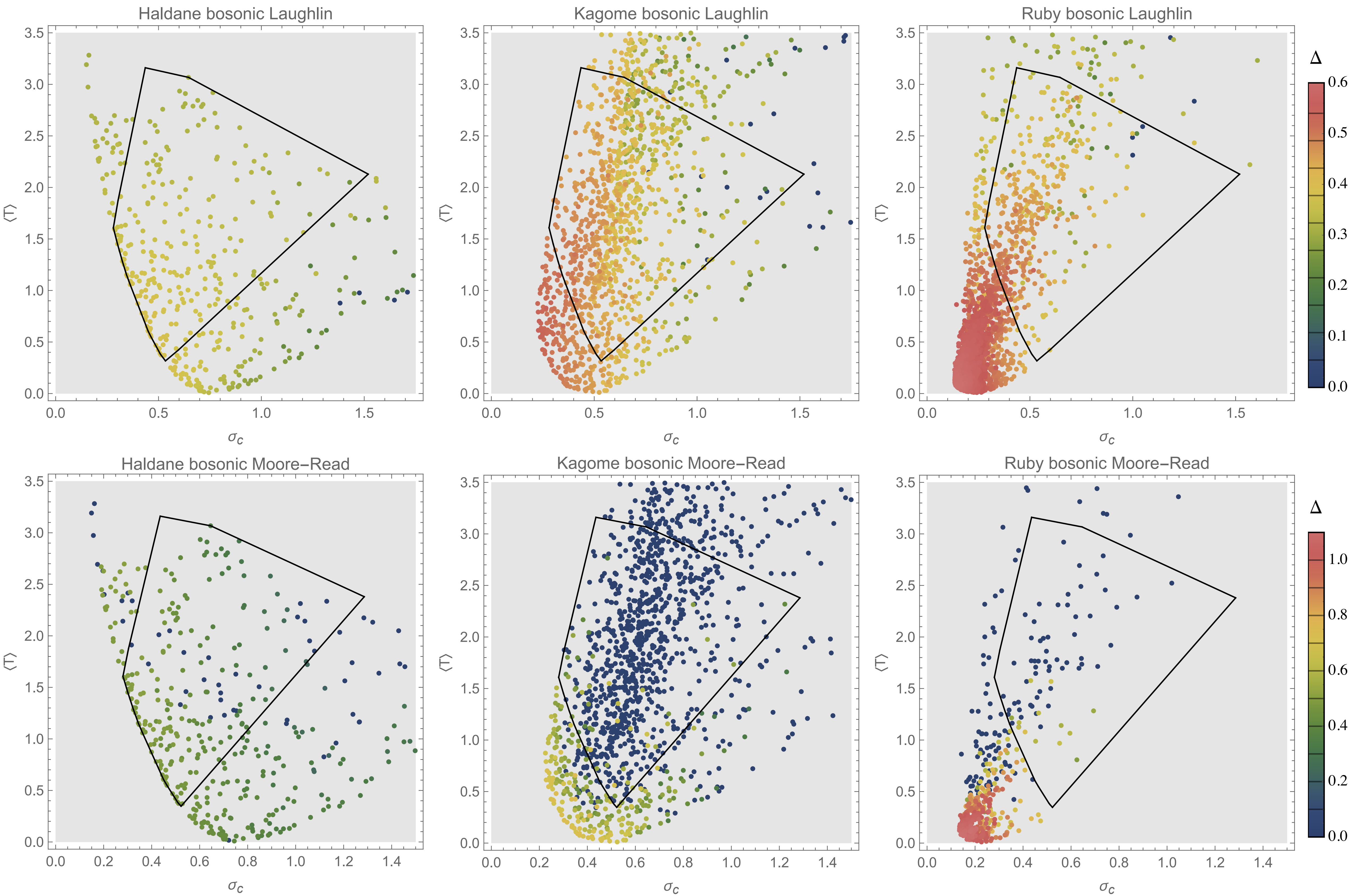

(New) data collapse restricted to points in common support

Red, green, blue are ruby, kagome and Haldane-t3
3 different views of same 3d scatterplot

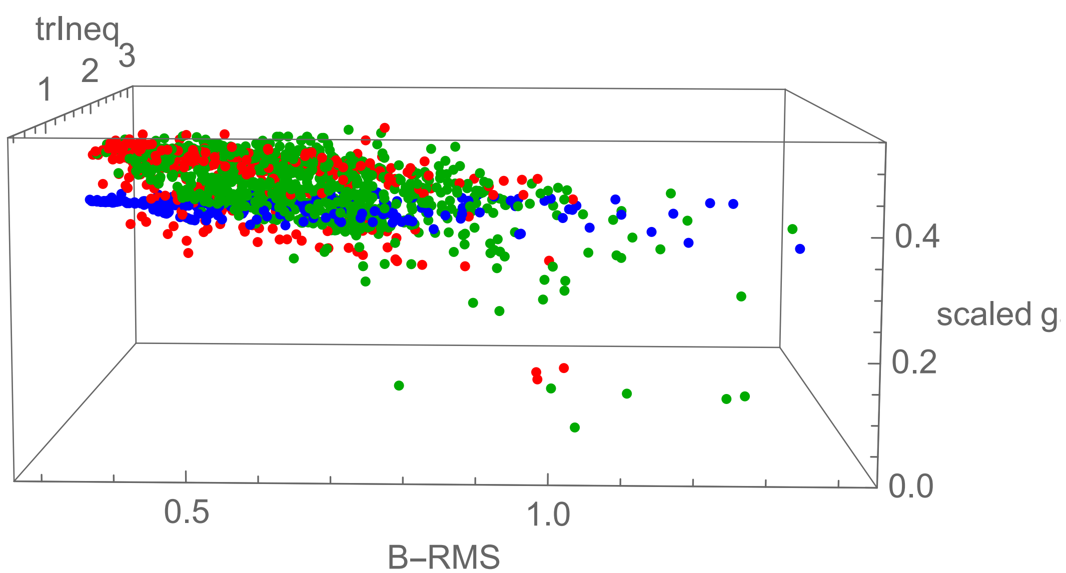

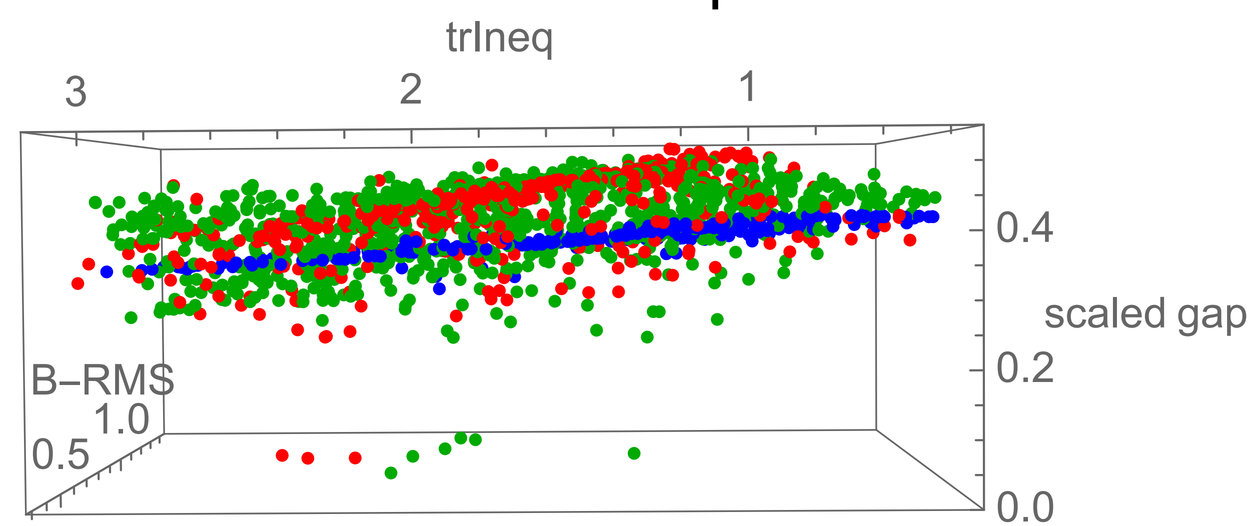

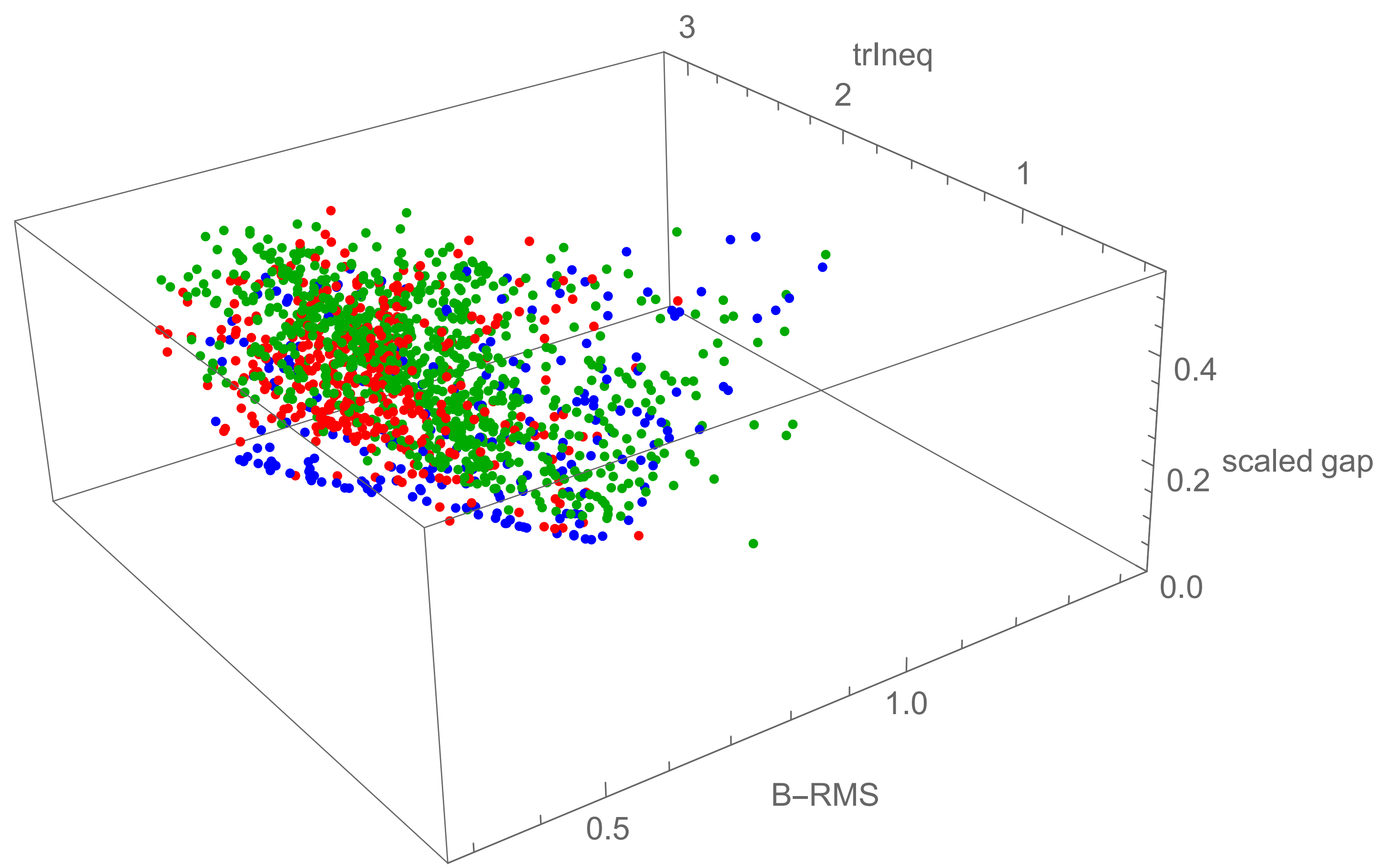

(New) data collapse restricted to points in common support

Red, green, blue are ruby, kagome and Haldane-t3

Surfaces generated from interpolated smoothed scaled gaps